^{11}C- and ^{18}F-Labeled tryptophans as PET-tracers for imaging of altered tryptophan metabolism in age-associated disorders

B.D. Zlatopolskiy[1,2,3], H. Endepols[1,2,4], R.N. Krasikova[5*], O.S. Fedorova[5], J. Ermert[2], B. Neumaier[1,2,3*]

[1] Forschungszentrum Jülich GmbH, Institute of Neuroscience and Medicine, Nuclear Chemistry (INM-5), 52425 Jülich, Germany;

[2] University of Cologne, Faculty of Medicine and University Hospital Cologne, Institute of Radiochemistry and Experimental Molecular Imaging, Cologne, Germany;

[3] Max Planck Institute for Metabolism Research, Cologne, Germany;

[4] University of Cologne, Faculty of Medicine and University Hospital Cologne, Nuclear Medicine Department, Cologne, Germany;

[5] N.P.Bechtereva Institute of the Human Brain, St.-Petersburg, Russia;

[*]Corresponging author

raisa@ihb.spb.ru;

b.neumaier@fz-juelich.de

Author's Information:

Boris Zlatopolskiy; senior scientist at the Institute of Radiochemistry and Experimental Molecular Imaging at the University Clinic of Cologne; Priv.-Doz., Ph. D.; translation of emerging synthetic methods to PET chemistry, development of novel radiotracers for diagnostics and staging of tumors and neurological disorders; boris.zlatopolskiy@uk-koeln.de.

Heike Endepols, head of the preclinical imaging group at the Institute of Radiochemistry and Experimental Molecular Imaging and the Department of Nuclear Medicine at the University Hospital Cologne; Adj. Prof., Ph. D.; preclinical PET imaging of neurodegenerative diseases and behavioral analysis; heike.endepols@uk-koeln.de.

Raisa Krasikova

Olga Fedorova

Johannes Ermert; deputy director of the Institute of Medicine and Neuroscience, INM-5: Nuclear Chemistry at the Forschungszentrum Jülich; Adj. Prof.; Ph. D; development of labeling methods for fluorine-18 and selenium-73; j.ermert@fz-juelich.de.

Bernd Neumaier; head of the Institute of Radiochemistry and Experimental Molecular Imaging at the University Clinic Cologne and director of the Institute of Medicine and Neuroscience, INM-5: Nuclear Chemistry at the Forschungszentrum Jülich; Univ. Prof., Ph. D., development of ^{18}F-fluorination strategies, production and separation of non-standard-radionuclides; b.neumaier@fz-juelich.de.

Abstract: The ageing of the world's populations is the result of increased life expectancy observed in almost all countries throughout the world. Consequently, a rising tide of aging-associated disorders, like cancer and neurodegenerative diseases, represents one of the main global challenges of the 21th century. The ability of mankind to overcome these challenges is directly dependent on the capability to develop novel methods for therapy and diagnostics of age-associated diseases. One hallmark of age-related pathologies is an altered tryptophan metabolism. Numerous pathological processes including neurodegenerative and neurological diseases like epilepsy, Parkinson's and Alzheimer's diseases, as well as cancer and diabetes exhibit marked changes in tryptophan metabolism. Visualization of key processes of tryptophan metabolic pathways, especially using positron emission tomography (PET) and related hybrid methods like PET/CT and PET/MRI, can be exploited to early detect the aforementioned disorders with considerable accuracy, allowing appropriate and timely treatment of patients. Here we review the published carbon-11 and fluorine-18 labeled tryptophans with respect to the production as well as preclinical and clinical evaluation as PET-tracers for visualization of different branches of tryptophan metabolism.

Table of CONTENT

1. Introduction

Higher life expectancy in almost all countries throughout the world leads to the aging of the population. Consequently, a rising tide of aging-associated disorders, like cancer and neurodegenerative diseases, represents one of the main global challenges of the 21st century. The ability of mankind to overcome these challenges is directly dependent on the capability to develop novel methods for therapy and diagnostics of age-associated diseases. One hallmark of age-related pathologies is an altered tryptophan metabolism. Tryptophan (Trp) is an essential proteinogenic amino acid, which contains an indole ring in the side chain. Although Trp is the least abundant amino acid in animal proteins (approx. 1.4%),[1] there are some Trp-rich proteins, such as the translocator protein 18 kDa (TSPO), which contain 6.8–7.7% Trp.[2] Apart from its incorporation into proteins, Trp serves mainly as a precursor for various metabolic pathways, which result in

different important biomolecules such as serotonin, melatonin, niacin (vitamin B3) and kynurenines.[3]

1.1. Kynurenine pathway

The kynurenine pathway is intimately linked to the immune system. It has been speculated that it has evolved as a defense strategy against viral and bacterial infections, based on tryptophan depletion.[4, 5] The initial step is the oxidative cleavage of the indole ring by tryptophan-2,3-dioxygenase (TDO) or indoleamine 2,3-dioxygenase (IDO), which converts Trp to *N*-formylkynurenine. The latter in turn is metabolized to kynurenine by kynurenine formamidase (Fig. 1). The two rate-limiting enzymes TDO and IDO are localized complementary, with TDO mainly expressed in the liver, and IDO in other tissues.[6, 7] TDO plays an essential role in the homeostasis of systemic Trp metabolism,[8] and oxidizes 90% of body Trp under physiologic conditions.[9] IDO is induced at sites of inflammation and infection, depleting Trp from the local microenvironment.[7] The kynurenine pathway metabolites regulate the immune response during pregnancy, cancer, inflammation and autoimmunity, but also with respect to commensal microorganisms, e.g. in the gastrointestinal tract. Kynurenine biosynthesis in the healthy brain is negligible.[10] Instead, peripheral kynurenine crosses the blood-brain barrier and is further metabolized into active metabolites predominantly by glial cells, but also to some degree by neurons. Under pathological conditions, IDO can be induced in microglia by interferon-γ-producing T helper cells.[11] Depending on the metabolic route, different kynurenine metabolites form, this can act either as anti-inflammatory and neuroprotective agents or as pro-inflammatory free radical generators.

Cerebral kynurenine can be metabolized via three different routes (Fig. 1):

(1) KAT-branch: Kynurenine aminotransferases (KAT) catalyze transamination of kynurenine to form kynurenic acid. The latter acts as an NMDA receptor antagonist, α7nACh receptor antagonist and free radical scavenger, and is considered neuroprotective. The KAT-branch is the predominant pathway in astrocytes.[12]

(2) KYNU-branch: Kynureninase (KYNU) metabolizes kynurenine to anti-inflammatory anthranilic acid. Owing to the low affinity of kynurenine to KYNU, metabolism via this branch occurs only at elevated kynurenine concentrations. Anthranilic acid is a potent inhibitor of 3-hydroxyanthranilate oxidase (3-HAO), preventing the formation of quinolinic acid via the KMO branch.[13]

(3) KMO-branch: This branch is the main route of the kynurenine pathway owing to the high affinity of kynurenine to kynurenine 3-monooxygenase (KMO). KMO metabolizes kynurenine to the free radical generator 3-hydroxykynurenine. 3-Hydroxykynurenine is in turn converted to a second free radical generator 3-hydroxyanthranilic acid by KYNU. This intermediate further undergoes non-enzymatic cyclization yielding the excitotoxic NMDA receptor agonist quinolinic acid. The latter is subsequently transaminated to generate niacin, and, finally, after several additional steps, NAD^+. Only microglia and macrophages produce quinolinic acid, while neurons predominantly synthesize the neuroprotective picolinic acid from 3-hydroxyanthranilic acid.[14]

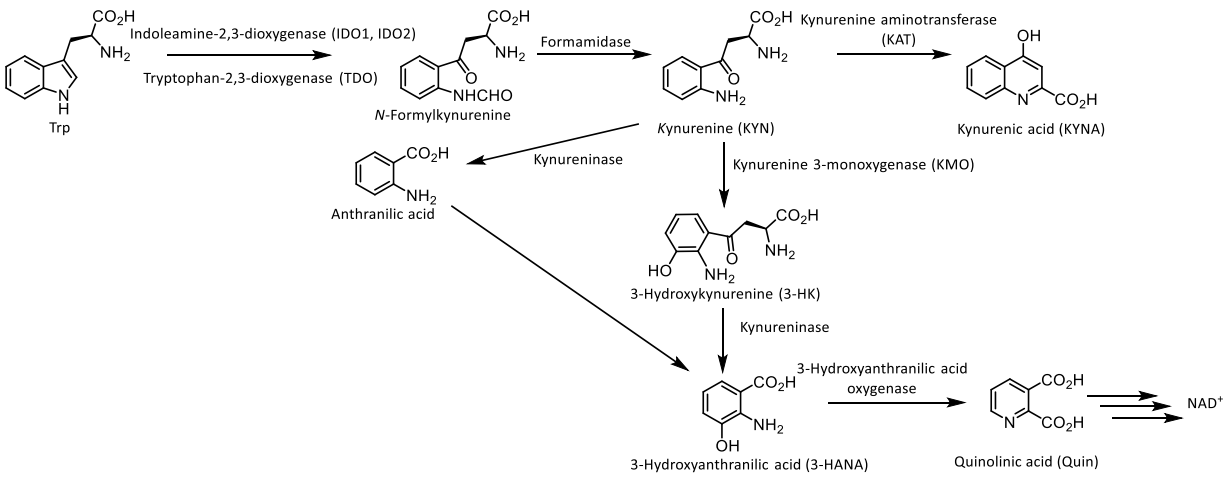

Figure 1: Kynurenine pathway.

1.2. Serotonin synthesis

Serotonin (5-hydroxytryptamine) is a signaling molecule which influences through regulation of sensory and motor processing, cognition and autonomous functions, all

essential systems in the brain.[15] The cell bodies of serotonergic neurons are localized in the brainstem raphe nuclei, and a dense network of axonal fibers covers all regions of the brain. While only 5% of body serotonin is produced in the brain, 95% is found in enterochromaffin cells in the gastrointestinal tract, where it plays a key role in sensory-motor and secretory functions as well as in immune cell activation.[16]

Serotonin is synthesized from tryptophan in two steps (Fig. 2): hydroxylation by tryptophan hydroxylase (TPH) followed by decarboxylation by aromatic amino acid decarboxylase (AADC).[17] TPH is the rate-limiting enzyme; it uses Fe^{2+} as a cofactor, as well as oxygen and tetrahydrobiopterin (BH_4) as co-substrates. In brain, activation of the kynurenine pathway usually leads to decreased serotonin synthesis ("kynurenine shunt").[18]. This is caused by reduction of the tryptophan pool available for serotonin synthesis owing to elevated IDO activity. Furthermore, under inflammatory conditions associated with activation of the KYN pathway, increased activity of the enzyme GTP-cyclohydroxylase-1 (GCH1) leads to a decreased level of BH_4, thus limiting TPH activity.[18]

No serotonin-degrading enzymes are present in the extracellular space. Consequently, serotonin reuptake is required before metabolization. In neurons, serotonin is deaminated by monoamine oxidase (MAO) affording 5-hydroxy-3-indolacetaldehyde (5-HIAL), which is further oxidized to 5-hydroxy-3-indolacetic acid (5-HIAA) by aldehyde dehydrogenase type 2 (ALDH2) or reduced to 5-hydroxytryptophol (5-HTOL) by aldehyde reductase (ALDR) or alcohol dehydrogenase (ADH). In the pineal gland, serotonin is first acetylated to form *N*-acetylserotonin by serotonin *N*-acetyltransferase, which is sequentially methylated by hydroxyindole-O-methyltransferase to form melatonin.[19] Melatonin is a regulatory molecule, best known for its influence on circadian rhythm and sleep promotion, but which also has numerous other functions related to energy metabolism and ageing.[20, 21]

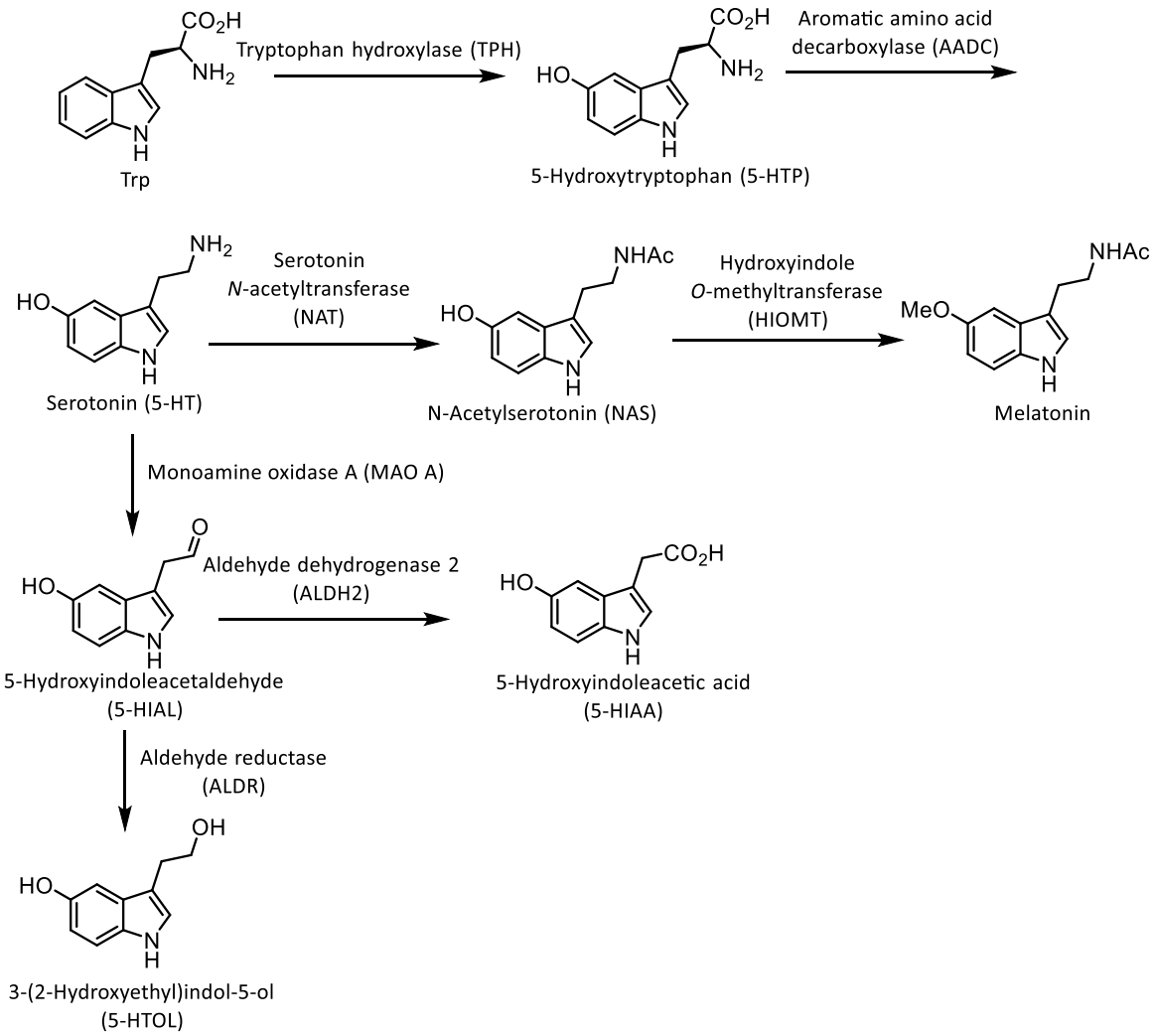

Figure 2: Serotonin pathways.

1.3. Rationale for PET-imaging of Trp metabolism

Visualization of different tryptophan metabolic pathways is highly relevant for clinical diagnostics owing to the involvement of Trp and its metabolites in different physiological and pathophysiological processes. For example, in neurodegenerative diseases, such as Alzheimer's and Parkinson's disease, serotonin synthesis is often significantly downregulated, while kynurenine metabolism is upregulated.[22-24] On the other hand, in numerous tumors, serotonin metabolism is strongly increased,[25] which is often accompanied by parallel upregulation of kynurenine metabolism used for tumor escape.[26] While serotonin and kynurenine metabolism in tumors can be in principle determined from tissue samples, this method is not applicable for monitoring the

progression of the disease (e.g. therapy response or formation of novel lesions), in the brain. The plasma kynurenine to tryptophan ratio is therefore frequently used as an indirect measure to estimate IDO activity.[27, 28] However, this ratio is influenced by numerous other factors[28] and is therefore not a reliable surrogate marker for IDO activity. In contrast, PET imaging can be used for the direct and repetitive measurenments of serotonin and kynurenine metabolism in the same individual. Furthermore, it could not only serve as a guiding tool for biopsy but also substantially improve diagnostic accuracy and, consequently, patient care.

Widespread implementation of molecular imaging techniques, especially positron emission tomography (PET) and related hybrid methods like PET/CT and PET/MRI in clinical practice have significantly contributed to a considerable increase of diagnostic accuracy in the last years. PET offers unique opportunities for a dynamic 3D-visualization of physiological and pathophysiological events *in vivo* on the molecular level. This imaging modality utilizes probes labeled with positron emitting nuclides (PET tracers) interacting specifically with molecular targets or biochemical processes of interest. PET imaging of Trp metabolism using ^{11}C-labeled Trp analogues has been shown to improve the accuracy of primary diagnostics, staging and therapy follow-up of tumors and neurological disorders.[29, 30] Nevertheless, the short half-life of ^{11}C ($t_{1/2}$ = 20 min), as well as the laborious and time-consuming procedures for the preparation of these tracers has prevented a broad implementation of Trp-PET in clinical practice. In contrast, ^{18}F possesses a half-life of 109.7 min, which is more suitable for both the synthesis and clinical application.

While numerous PET tracers specific for serotonin receptors and transporters have been developed,[31] tracers for the visualization of serotonin synthesis and/or activity of the KYN pathway are still rarely found.

Herein we review the published ^{11}C- and ^{18}F-labeled Trp-based radiotracers, and analyze their suitability to target the kynurenine and/or the serotonin branches of Trp metabolism. Furthermore, we briefly discuss the potential of ^{11}C- and ^{18}F-labeled Trp analogs as PET probes for imaging of altered tryptophan metabolism in neurological and oncological diseases.

2. ^{11}C-Labeled tryptophans and tryptophan analogs

Carbon-11 is usually produced at a low energy cyclotron via the $^{14}N(p,\alpha)^{11}C$ nuclear reaction. The target N_2-gas contains either 0.5% of oxygen or 5% of hydrogen. This leads directly to the formation of [^{11}C]carbon dioxide or [^{11}C]methane, respectively. Known synthetic methods for the construction of the indole ring are not suitable for ^{11}C-labeling owing to the short half-life of carbon-11.[32] Consequently, ^{11}C could be introduced only in carboxyl-, αCH- or CH_2-groups of Trp.

2.1. Racemic 1-[^{11}C]- and 5-hydroxy-1-[^{11}C]tryptophans

Preparation of the racemic 1-[^{11}C]Trp via Bucherer-Bergs reaction

Washburn et al. prepared D,L-[^{11}C]Trp by the hydrolysis of the corresponding ^{11}C-labeled hydantoin with NaOH at 245 °C for 10 min. The radiolabeled intermediate was produced by the multicomponent Bucherer-Bergs reaction [33] of the 3-indolylacetaldehyde bisulfite adduct, $(NH_4)_2CO_3$, and NH_4Cl with carrier-added H[^{11}C]CN at 250 °C for 3 min (Fig. 3).[34, 35] Radiochemical yields (RCYs) starting from H[^{11}C]CN amounted to 35–55% with a specific activity of 0.55–1.1 GBq/mg. The synthesis time was 40-50 min. H[^{11}C]CN was synthesized by a catalytic reaction of [^{11}C]CH_4 and anhydrous NH_3 on Pt/Al at 950 °C.[36] Zalutski et al. published the improved protocol which allowed to produce D,L-1-[^{11}C]Trp from H[^{11}C]CN in a RCY of 50% within 28 min.[37]

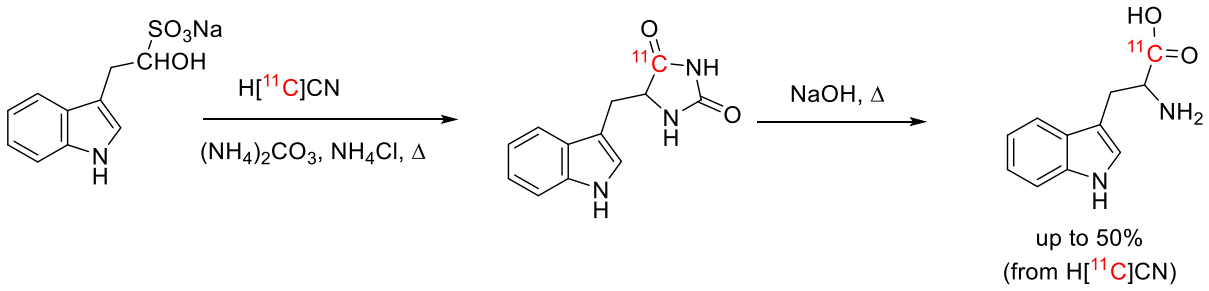

Figure 3: Preparation of the racemic 1-[^{11}C]Trp via Bucherer–Bergs reaction.

2.2. Chemoenzymatic synthesis of ^{11}C-labeled tryptophans

The Bucherer-Bergs synthesis, using ^{11}C-labeled cyanide, produced a racemic mixture of 1-[^{11}C]Trp. Since radiolabeling occurs in the carboxy position, radioactivity will be lost as [^{11}C]CO_2 during the first, decarboxylation, step of the serotonin biosynthesis. Correspondingly, methods allowing preparation of 2-[^{11}C]Trp were developed.
Enzymatic reactions enable fast stereoselective synthesis of amino acids under very mild conditions. Not surprisingly, they were intensely used for the preparation of amino acids labeled with short-lived isotopes like ^{11}C and ^{13}N.[38-41]

L-[2-^{11}C]-, 5-hydroxy-L-[2-^{11}C]- and 5-fluoro-L-[2-^{11}C]tryptophans ([2-^{11}C]Trp, 5-OH-[2-^{11}C]Trp and [2-^{11}C]5-FTrp)

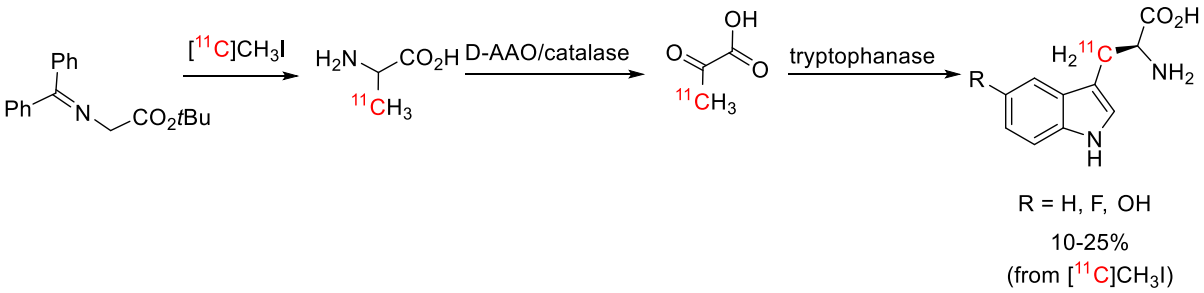

Figure 4: Preparation of L-[2-^{11}C]-, 5-hydroxy-L-[2-^{11}C]- and 5-fluoro-L-[2-^{11}C]tryptophans using chemoenzymatic synthesis.

L-[2-^{11}C]-, 5-hydroxy-L-[2-^{11}C]- and 5-fluoro-L-[2-^{11}C]tryptophans were prepared from racemic [3-^{11}C]alanine using two consecutive enzyme-catalyzed transformations, which were carried out in a one-pot manner (Fig. 4).[42, 43] First, *N*-(diphenylmethylene)glycine *tert*-butyl ester was labeled with [^{11}C]methyl iodide affording after hydrolysis of the intermediate labeled imine ester DL-[3-^{11}C]Ala which in turn was deaminated into 3-[^{11}C]pyruvic acid using D-amino acid oxidase (DAO), catalase (CAT) and glutamic pyruvic transaminase (GPT).[44] In the subsequent step 3-[^{11}C]pyruvic acid was converted into enantiomerically pure L-[2-^{11}C]-, 5-hydroxy-L-[2-^{11}C]- and 5-fluoro-L-[2-^{11}C]tryptophans by the reversed tryptophanase reaction with indole, 5-hydroxy- or 5-fluoroindole, respectively.[42] The total synthesis time starting from [^{11}C]methyl iodide including HPLC purification was 50–70 min, RCYs of tracers in a ready-to-use form amounted to 10–25%. The application of a column packed with the corresponding

enzymes immobilized on a solid support[45] enabled implementation of the chemoenzymatic synthesis of 5-hydroxy-L-[2-^{11}C]tryptophan into automated synthesis modules.[45, 46] Furthermore, the production 5-OH-[2-^{11}C]Trp using a commercially available robotics system was also established.[47, 48] However, the exceptional complexity of the proposed four-step preparation procedures (starting from [^{11}C]CO_2 or [^{11}C]CH_4), which include the enzymatic steps, where four enzymes and the appropriate coenzymes are used, and which require exact concentration of the applied reagent and exact adjustment of pH, obviates a widespread application of this tracer.5-Hydroxy-L-tryptophan is the direct precursor of serotonin. Consequently, 5-OH-[2-^{11}C]Trp also enters the serotonin metabolic pathway.[49] 5-Hydroxy-[2-^{11}C]tryptamine (^{11}C-labeled serotonin) and its metabolite 5-hydroxy-[2-^{11}C]indoleacetic acid ([^{11}C]HIAA) were identified as main metabolites in humans, monkeys and rodents. However, 5-OH-[2-^{11}C]Trp strongly accumulates in basal ganglia,[50, 51] suggesting unspecific uptake in dopaminergic and noradrenergic presynaptic terminals because of the high affinity of 5-OH-Trp to AADC. Furthermore, in the case of activated kynurenine metabolism, e.g., by neuroinflammation, 5-OH-[2-^{11}C]Trp can also to some extent be metabolized by IDO, although with K_m 20 times lower compared to L-tryptophan.[52] Despite these limitations, 5-hydroxy-[2-^{11}C]tryptophan has been occasionally used for imaging of the serotonergic system in patients suffering from neuropsychiatric diseases such as social anxiety disorders,[53] dysphoria[54] and depression.[55] Furthermore, this tracer is able to visualize degeneration of serotonin-producing pancreatic islet cells in diabetic patients.[56] In rodents, contradictory results have raised doubt regarding the suitability of 5-OH-[2-^{11}C]Trp as a marker for quantification of serotonin synthesis.[57] AADC inhibition did not affect kinetic constants, suggesting that trapped radioactivity comprises mainly unmetabolized radiotracer. In contrast, while 5-hydroxy-[2-^{11}C]tryptophan is not a substrate of tryptophan hydroxylase, inhibition of this enzyme reduced its brain uptake and decarboxylation.[57] The main application field of 5-OH-[2-^{11}C]Trp remains detection of serotonin-producing neuroendocrine tumors,[58] originating mainly from neuroendocrine cells of the pancreatic islets, gastrointestinal tract and bronchopulmonary system.[59] Tracer accumulation in tumor cells is influenced by L-

amino acid transporters (LATs) as well as AADC and MAO activity.[60] 5-Hydroxy-[2-^{11}C]tryptophan was particularly effective in staging of islet cell tumors.[61]

5-Fluoro-[2-^{11}C]tryptophan was evaluated *in vitro* in a neuroendocrine tumor cell line and *in vivo* in normal rats, in neuroendocrine tumor xenografts bearing mice and in a non-primate monkey.[43] This study demonstrated that [2-^{11}C]5-FTrp is a functional analogue of 5-OH-[2-^{11}C]Trp *in vitro*. However, results of animal experiments suggested that this tracer did not target serotonin metabolism *in vivo*.

Chemoenzymatic synthesis of [carboxy-^{11}C]- and 5-hydroxy-[carboxy-^{11}C]tryptophans ([1-^{11}C]Trp and 5-HO-[1-^{11}C]Trp)

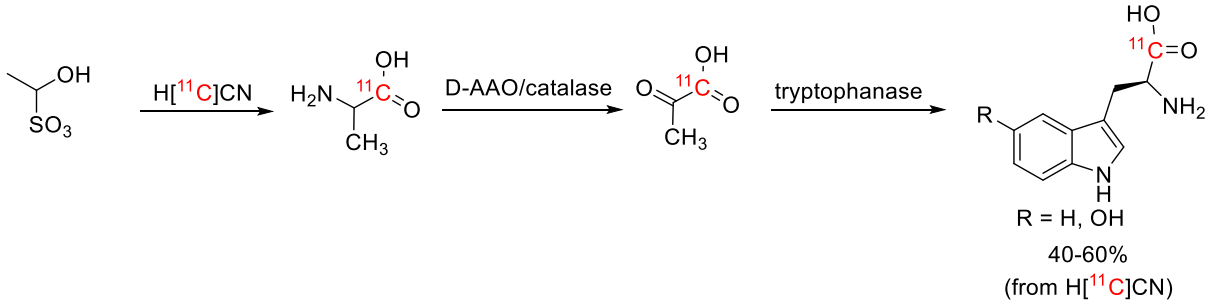

Figure 5: Chemoenzymatic synthesis of [carboxy-^{11}C]- and 5-hydroxy-[carboxy-^{11}C]tryptophans.

[1-^{11}C]Trp and 5-HO-[1-^{11}C]Trp were synthesized starting from [1-^{11}C]alanine ([1-^{11}C]Ala) using the same chemoenzymatic protocol as for the production of these amino acids labeled in the β-position. Racemic [1-^{11}C]Ala was obtained by the addition of H[^{11}C]CN to ammonia and bisulfite adduct of acetaldehyde and subsequent hydrolysis of the resulting [^{11}C]aminonitrile (Fig. 5).[62] 1-^{11}C-Labeled amino acids were prepared in RCYs of 40–60%, based on [^{11}C]cyanide, in total synthesis time of 50 min.

When tryptophan analogues are ^{11}C-labeled in the carboxyl position, ^{11}C is cleaved off by AADC in the form of $^{11}CO_2$, which is eliminated through the lungs. Neuroendocrine tumors, which were successfully visualized with 5-hydroxy-[2-^{11}C]tryptophan, could therefore not be delineated by 5-hydroxy-L-[carboxy-^{11}C]tryptophan.[63]

2.3. ^{11}C-Methylated tryptophans

^{11}C-Alkylation, especially the ^{11}C-methylation, is definitely the most popular method for the preparation of ^{11}C-labeled compounds. ^{11}C-Methylation is mainly carried out using [^{11}C]methyl iodide as alkylating agent. The latter is widely used for the preparation of different PET-tracers like [^{11}C]acetate, [^{11}C]carfentanil, [^{11}C]choline, [^{11}C]methionine, [^{11}C]Pittsburgh Compound B ([^{11}C]PiB), [^{11}C]raclopride and others.[64] This radiolabeled building block can be easily prepared in preparative scale virtually in any commercially available automated synthesis module suitable for ^{11}C-labeling.

[^{11}C]CH_3I can be produced using two different methods. According to the so called "wet" method, cyclotron produced [^{11}C]CO_2 is reduced by $LiAlH_4$ to [^{11}C]methanol, which is subsequently converted to [^{11}C]CH_3I by the treatment with hydrogen iodide[65] or triphenylphosphine diiodide.[66] Alternatively, according to the so called "dry" method, [^{11}C]methane is reacted with I_2 at 720–740 °C affording [^{11}C]methyl iodide.[67, 68] [^{11}C]CH_4 is usually prepared by the hydrogenation of [^{11}C]CO_2 trapped on molecular sieves in the presence of a Ni catalyst at 400 °C.

α-[^{11}C]Methyltryptophan ([^{11}C]AMT)

[^{11}C]AMT remains the most popular PET probe for the visualization of Trp metabolism.[49] Initially, this tracer was produced starting from methyl 3-(indol-3-yl)-2-[(phenylmethylidene)amino]propanoate, accessible in one step from H-Trp-OMe and benzaldehyde, as follows.[69] Achiral enolate generated by the treatment with LDA was quenched with [^{11}C]methyliodide to give the corresponding radiolabeled intermediate which was deprotected with 2 M HCl at 135 °C for 5 min affording the desired radiotracer in a non-decay corrected (n.d.c.) yield of 20–30% within 30 min total synthesis time with Trp as the only impurity (Fig. 6). Noteworthy, no side product originating from N_{in}-alkylation was observed. While the authors initially assumed that [^{11}C]AMT was prepared as a single L-enantiomer, further investigations failed to confirm this point.[70, 71]

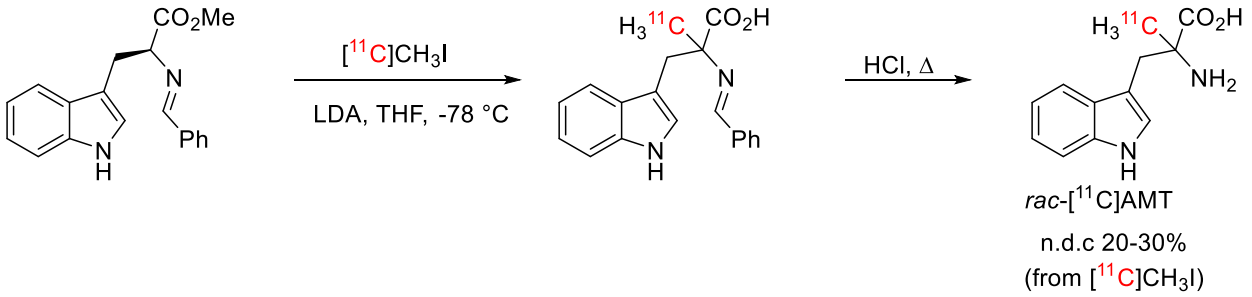

Figure 6: Preparation of racemic [^{11}C]AMT starting from benzaldimine of Trp-OMe.

Suehira et al.[70] modified the original procedure by increasing the reaction temperature for the deprotonation step to 25–30 °C. This allowed to reduce the reaction time from 20 to 5 min. Additionally, the deprotection step was optimized as follows. Instead of the low-efficient one-step acidic deprotection of the ^{11}C-labeled intermediate, the radiolabeled benzaldimine was first cleaved by a brief treatment with 1 M HCl at 105 °C and the resulting [^{11}C]AMT methyl ester was hydrolyzed using 2 M NaOH to provide racemic [^{11}C]AMT. Finally, HPLC purification delivered the desired tracer in a RCY of 25–30% within 25 min starting from [^{11}C]iodomethane.

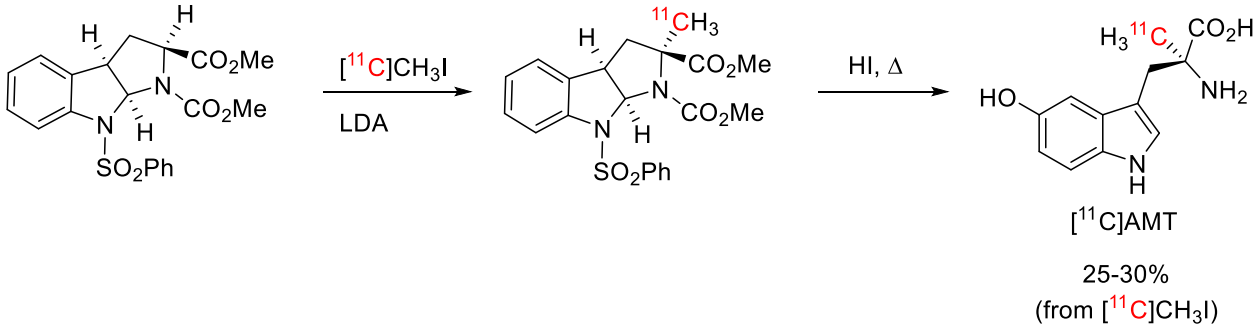

Figure 7. Preparation of α-[^{11}C]methyltryptophan.

α-[^{11}C]Methyltryptophan was prepared from the chiral enolate generated from the fully protected tricyclic Trp derivative, dimethyl (2*S*,3a*R*,8a*S*)-8-(phenylsulfonyl)-3,3a,8,8a-tetrahydropyrrolo[2,3-b]indole-1,2(2*H*)-dicarboxylate, using LDA and [^{11}C]CH_3I followed by hydrolysis with 57% HI at 200 °C for 5 min and HPLC purification (Fig. 7). Using this procedure, enantiomerically pure [^{11}C]AMT (*ee* ~ 97%) was synthesized

in a RCY of 36% within 22 min starting from [^{11}C]CH_3I.[72] In order to avoid application of highly corrosive HI, the ^{11}C-labeled tricyclic intermediate was first treated with TFA followed by removal of all volatiles under reduced pressure and thereafter the residue was heated with 10 N NaOH at 210 °C for 10 min.[71, 73] Finally, neutralization of the reaction mixture with H_2SO_4 followed by HPLC purification afforded the PET-tracer in 22% n.d.c. RCY within 40 min starting from [^{11}C]CH_3I. Despite being very cumbersome (four reaction and six operation steps) the procedure was successfully transferred to an automated synthesis module for *c*GMP production of the tracer.[74, 75] Furthermore, based on this protocol, Chakraborty et al. developed a procedure for the production of [^{11}C]AMT, which avoided the HPLC purification step.[73] Instead, reversed phase solid phase extraction (SPE) purification was applied. Unfortunately, published protocols for the automated production of [^{11}C]AMT entail strictly anhydrous/oxygen-free conditions and low temperatures (–55 to –20 °C). These requirements cannot be fulfilled using commercially available modules, preventing a broader broader application of [^{11}C]AMT.

As already mentioned α-[^{11}C]methyltryptophan has been extensively used for diagnostic imaging. It is not a substrate for protein synthesis, and is trapped in the brain because its metabolite α-[^{11}C]methylserotonin is not degraded by monoamine oxidase.[76] Experiments with α-[^{14}C]methyltryptophan have shown that radioactivity is still detectable in the brain after 5 days.[77] Whereas α-[^{11}C]methyltryptophan is considered a highly reproducible surrogate marker for serotonin synthesis,[78, 79] the presence of a large pool of radioactivity irreversibly trapped in brain tissue complicates the quantification of serotonin biosynthesis.[30] This could be presumably explained by the fact that α-methyltryptamine, the product of decarboxylation of AMT by AADC, is an inhibitor of monoamine oxidase A.[80] The latter is widely expressed in different brain regions.[81] Nevertheless, [^{11}C]AMT has been used to study the serotonergic system in depressive disorders,[82-84] obsessive-compulsive disorder,[85, 86] Tourette syndrome,[87] drug abuse[88] and migraine.[89] However, under pathological conditions which involve brain inflammation, the kynurenine pathway metabolizes a considerable amount of tryptophan in the brain[30],which cannot be distinguished with α-[^{11}C]methyltryptophan. The main field of application of this tracer is therefore localization of epileptogenic tissue [90, 91] and

brain tumors,[92-94] both based on strong kynurenine pathway activations exceeding by far possible down regulation of serotonin metabolism. In a preliminary multimodal glioblastoma study with 30 patients, the higher [^{11}C]AMT uptake within MRI contrast-enhancing tumor sub-regions was highly predictive for longer overall survival.[95]

Although there is a clear association between α-[^{11}C]methyltryptophan uptake and activity of the kynurenine pathway, *in vitro* studies suggest that α-[^{11}C]methyltryptophan is not metabolized by IDO.[96] It seems that [^{11}C]AMT accumulation is caused by up-regulation of a tryptophan selective transporter, induced by IDO expression[97] rather than by entering the kynurenine pathway.

An example where both serotonin synthesis and kynurenine pathway activity are elevated in parallel is breast cancer. Extensive tumoral tryptophan degradation can deplete the body of tryptophan, leading to reduced cerebral serotonin synthesis and hence tumor-induced depression,[98] It is therefore not surprising that breast cancer cells strongly accumulate α-[^{11}C]methyltryptophan. In contrast to gliomas and lung cancers, most breast cancers show a rapid tracer influx and an early peak (less than 20 min after injection) followed by a subsequent decline of radioactivity uptake.[99] [^{11}C]AMT kinetic analysis can therefore be employed to differentiate tumor types, e.g. glioblastomas from metastatic brain tumors.[100, 101]

L- and D-N_{in}-[^{11}C]Methyltryptophans (L- and D-[^{11}C]1MTrps)

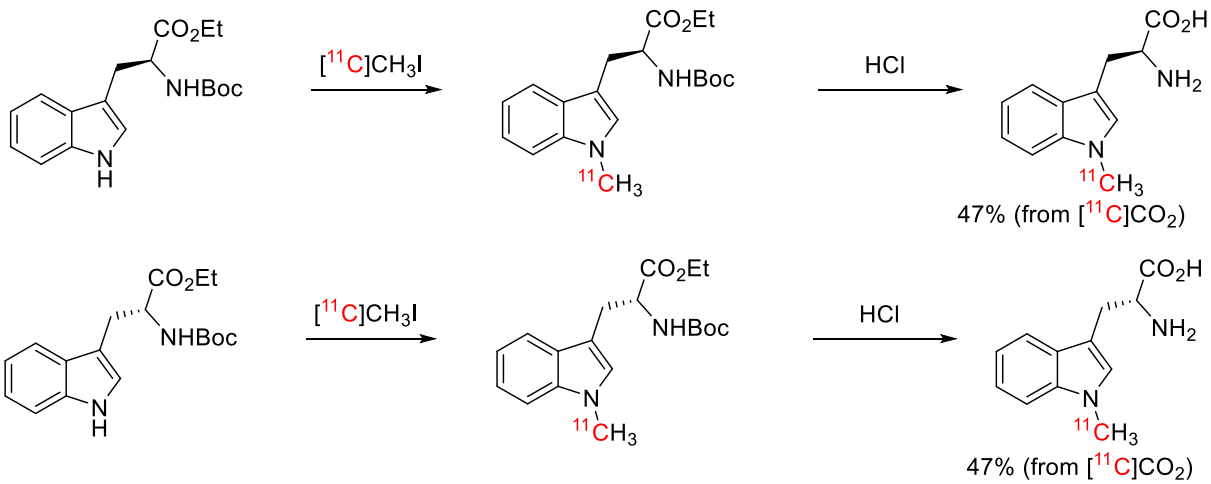

Figure 8: Preparation of L- and D-N_{in}-[^{11}C]methyltryptophans (L- and D-[^{11}C]1MTrps).

L-N_{in}-Methyltryptophan (L-1MTrp) is a known concurrent inhibitor of IDO1[102] and could be potentially used for the visualization of Trp metabolism via the kynurenine pathway. In contrast, the D-isomer (Indoximod) did not exert a significant inhibition of IDO1 in the cell-free enzyme assay. However, this isomer demonstrated superior anticancer activity in mouse xenografts of IDO-positive solid tumors and is currently being evaluated in several stage 1b/2 clinical trials as a single agent or in combination with other therapeutics, or with radiotherapy.[103, 104]

N-Methylation of Boc-L-Trp-OEt or Boc-D-Trp-OEt with [^{11}C]CH_3I, using NaOH as a base, followed by deprotection with HCl and, finally, by HPLC purification afforded L- and D-[^{11}C]1MTrps in 47% RCY based on [^{11}C]CO_2 within 40 min (Fig. 8).[105] Noteworthy, some racemization was observed during the alkylation step and enantiomeric excess (*ee*) of both stereoisomers amounted to~90%.

Biodistribution of L- and D-[^{11}C]1MTrps in normal rats was evaluated *in vivo* using μPET and *ex vivo* tissue sampling. In the case of the L-isomer the highest radioactivity accumulation was observed in pancreas, presumably in IDO1 positive β-cells.[106] In contrast, for D-[^{11}C]1MTrp the main target tissue were the kidneys whereas pancreas uptake was low.

3. ^{18}F-Labeled tryptophan analogs

To date most of the published preclinical and clinical PET-studies were carried out with ^{11}C-labeled tryptophans. The vast majority of such radiotracers could be prepared only using cumbersome and time-consuming multistep preparation procedures (*vide supra*). This together with the short half-life of ^{11}C (20.4 min) precludes broad evaluation of ^{11}C-labeled Trps and their implementation into clinical practice.

In contrast, the half-life of ^{18}F (109.8 min) in comparison to ^{11}C and the majority of other common PET nuclides like ^{15}O, ^{13}N and ^{68}Ga is much longer, and allows the accomplishment of demanding production procedures and long-lasting biological experiments (up to 6 h). Furthermore, the half-life of ^{18}F enables the commercialization of ^{18}F-labeled probes and their shipping to remote destinations (satellite concept). No

carrier added (n.c.a) nucleophilic [^{18}F]fluoride can be produced in a > 100 GBq scale at low-energy cyclotrons from [^{18}O]H_2O using the high-yielding ^{18}O(p,n)^{18}F nuclear reaction. Electrophilic [^{18}F]F_2 could be prepared from ^{20}Ne and $^{18}O_2$ via the ^{20}Ne(d,α)^{18}F and ^{18}O(p,n)^{18}F nuclear reactions. In order to prevent the adsorption of fluorine-18 produced in the highly reactive atomic form on the target walls, the addition of F_2 to the target gas is mandatory. Consequently, only carrier added (c.a.) [^{18}F]F_2 with low specific activity can be produced.[107-110] Fluorine-18 possesses outstanding decay properties that are ideally suited for PET imaging. The β^+ decay ratio of ^{18}F amounts to 97%. The energy of these positrons is relatively low [$E(\beta^+)_{max}$ = 630 keV]. Therefore, image blurring caused by travelling of the emitted particles in tissue before annihilation is also low.[111, 112]

3.1 **Preparation of 5-hydroxy-4-[^{18}F]fluoro- and 5-hydroxy-6-[^{18}F]fluorotryptophans (5-OH-4-[^{18}F]FTrp and 5-OH-6-[^{18}F]FTrp) by electrophilic radiofluorination**

5-Hydroxy-4-[^{18}F]fluoro- and 5-hydroxy-6-[^{18}F]fluorotryptophans remain the only radiolabeled tryptophan analogs produced by electrophilic radiofluorination. They were prepared by the reaction of 5-hydroxytryptophan (5-OHTrp) with [^{18}F]F_2 in anhydrous HF at –70 °C (Fig. 9). The mixture of regioisomeric ^{18}F-labeled amino acids was, after evaporation of HF, separated by HPLC furnishing 5-OH-4-[^{18}F]FTrp and 5-OH-6-[^{18}F]FTrp in RCYs of 7% and 9%, respectively.[113]

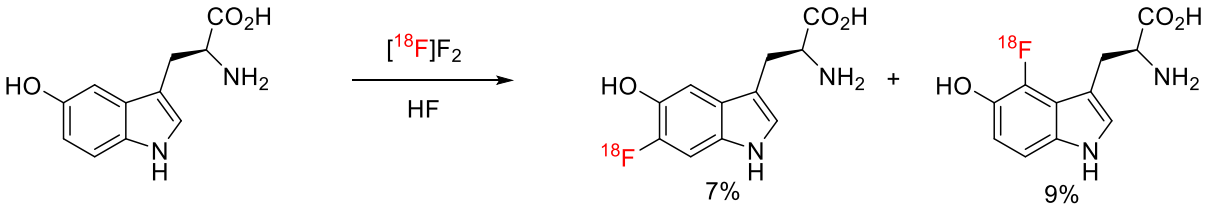

Figure 9: Preparation of 5-hydroxy-4-[^{18}F]fluoro- and 5-hydroxy-6-[^{18}F]fluorotryptophan (5-OH-4-[^{18}F]FTrp and 5-OH-6-[^{18}F]FTrp) via direct electrophilic radiofluorination of 5-hydroxytryptophan (5-OHTrp).

3.2 L- and D-1-(2-[^{18}F]Fluoroethyl)tryptophans (L- and D-1-[^{18}F]FETrps): preparation by S_N2 ^{18}F-fluorination and biological evaluation

Synthesis of tryptophan analogs with a ^{18}F-substituent on the indole ring using conventional radiofluorination protocols is complicated owing to the extremely electron rich and oxidation sensitive nature of the indole ring. In contrast, the efficient protocols for S_N2 ^{18}F-fluorination especially at primary carbons are well-established. Accordingly, numerous [^{18}F]fluoroalkyl-and [^{18}F]fluoroalkoxytryptophans were produced and evaluated.[114-120] However, Trp analogs containing bulky [^{18}F]fluoroalkoxy or [^{18}F]fluoroalkyl substituents are not able to target Trp metabolism and were evaluated as imaging agents for the visualization of the increased activity of LAT system in tumor lesions.[121,122,123] The only exception of this observation known so far represents L-1-(2-[^{18}F]fluoroethyl)tryptophan (L-1-[^{18}F]FETrp). Henrottin et al. demonstrated in cell-free enzymatic assays that 1-FETrp is a substrate of recombinant hIDO although with a much slower oxidation rate in comparison to Trp, 1-MTrp and 5-OHTrp (360×, 6× and 3×, respectively).[96]

Sun et al. produced 1-[^{18}F]FETrp by the alkylation of Boc-Trp-OEt with 1-[^{18}F]fluoro-2-(tosyloxy)ethane using NaOH as a base followed by deprotection of the radiolabeled intermediate with 8 M HCl at 100 °C in a n.d.c. RCY of 1% within a synthesis time of 65 min (Fig. 10A).[117] The enantiomeric purity of the tracer was not determined.

Henrottin et al. developed an improved procedure for the preparation of racemic 1-[^{18}F]FETrp.[118] Accordingly, Boc-Trp[Et(OTos)]-O*t*Bu was radiolabeled using [^{18}F]KF/K_2CO_3/Kryptofix®222 (K2.2.2) followed by deprotection with 6 M HBr at 90 °C for 10 min and HPLC isolation of the desired radiotracer (Fig. 10B). This protocol was implemented on a GE FASTlab synthesis module. The automated synthesis afforded 1-[^{18}F]FETrp in a RCY of 30% within 80 min. The racemic mixture after HPLC purification could be separated using two consecutive enantioselective HPLC separations to yield L- and D-1-[^{18}F]FETrps after formulation as injectable solutions in RCYs of 6% within 155 and 180 min of total synthesis time. A further optimization of this procedure allowed Xin and Cai to produce L- and D-1-[^{18}F]FETrps in a FX-N synthesis module in RCYs of 19 and 9%, respectively, within 90 min (Fig. 10C).[124].

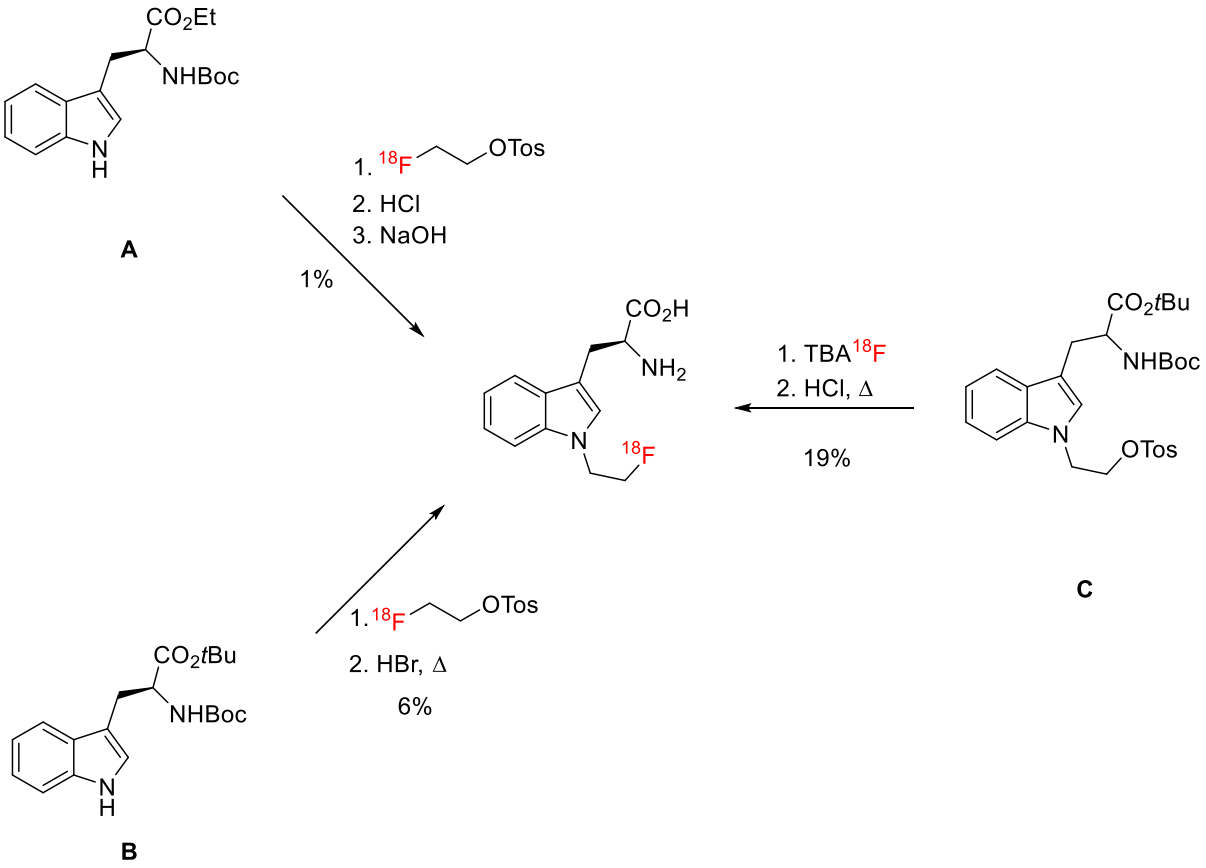

Figure 10. Preparation of 1-[^{18}F]FETrp according to Sun et al. (A [117]), Henrottin et al. (B [118]) and Xin and Cai (C [124]).

1-L-[^{18}F]FETrp highly accumulated in IDO-expressing cell lines. This uptake could be inhibited by 1-MTrp.[124] Additional inhibition studies showed that 1-L-[^{18}F]FETrp is a substrate of LAT-1 and ASC (alanine-, serine-, and cysteine-preferring) systems.[124] At the same time cellular uptake of D-1-[^{18}F]FETrp was negligible in all tested cell lines although it was a hIDO substrate in cell-free assays.[124] These results suggest much lower intracellular transport of the D- compared to the L-isomer. 1-L-[^{18}F]FETrp highly accumulated in different subcutaneous and orthotropic tumors in rodents allowing their visualization with high tumor-to-background ratio.[125] In a µPET study racemic 1-[^{18}F]FETrp was compared to [^{11}C]AMT in mice implanted with patient-derived brain tumor xenografts.[126] In this study 1-[^{18}F]FETrp demonstrated high stability towards defluorination and favorable radiation dosimetry. In contrast to [^{11}C]AMT, 1-[^{18}F]FETrp showed prominent uptake in the pancreas, presumably, in IDO-positive β-

cells. Furthermore, in all three studied tumor types tumoral SUV for 1-[^{18}F]FETrp was higher compared to [^{11}C]AMT. Additionally, 1-L- and D-[^{18}F]FETrps were evaluated in spontaneous medulloblastoma tumors in transgenic mice.[127] Whereas 1-L-[^{18}F]FETrp-PET enabled clear delineation of tumors from normal brain tissue, tumor accumulation of the D-tracer was low.

3.3. [^{18}F]Fluorotryptophans labeled in aromatic positions

Synthesis of c.a. racemic 5- and 6-[^{18}F]fluorotryptophans (5- and 6-[^{18}F]FTrps) using the Balz-Schiemann reaction and their preliminary biological evaluation

The Balz-Schiemann reaction is a conversion of (hetero)aryl amines to aryl fluorides via diazotisation and subsequent thermal decomposition of the derived tetrafluoroborates [128]. Historically, it was the first method applied for the ^{18}F-labeling of aromatic amino acids using [^{18}F]fluoride.[129] Since the ^{18}F-label was initially introduced in the tetrafluoroborate anion, the maximum possible radiochemical yield amounts to 25%. 5- and 6-[^{18}F]Fluorotryptophans were produced via pyrolysis of the corresponding 3-(3-ethoxy-2-(ethoxycarbonyl)-2-formamido-3-oxopropyl)-1*H*-indole-diazonium tetrafluoroborates in the presence of [^{18}F]HF followed by deprotection/decarboxylation of the corresponding labeled intermediates to afford 5- and 6-[^{18}F]FTrps in RCYs of 6–13% (Fig. 11).[130] Extremely low specific activities (12–23 MBq/g), low RCYs, very long preparation times of 220–255 min and, especially, the potentially explosive nature of diazonium salts impeded the further development of this method.

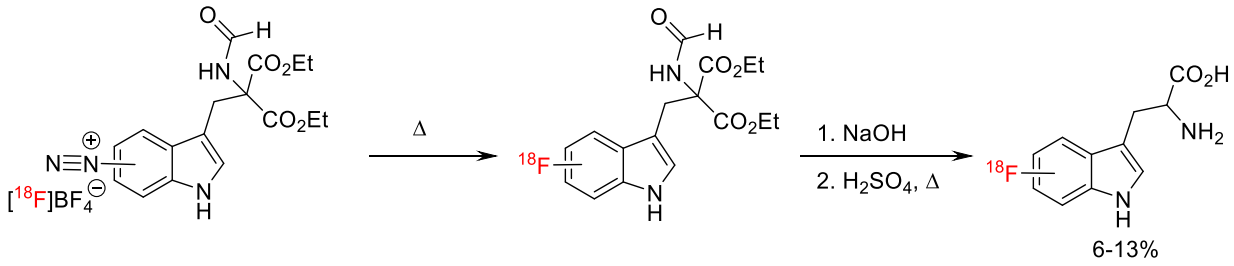

Figure 11: Preparation of 5- and 6-[^{18}F]FTrps from the corresponding diazonium tetrafluoroborate salts.

Preparation of 4-[^{18}F]fluoro-L-tryptophan (4-[^{18}F]FTrp) by isotopic exchange using carbonyl as transient activating group

The conventional procedure for S_NAr ^{18}F-fluorination necessitates the presence of a suitable leaving group like halogens, nitro or *N*,*N*,*N*-trimethylammonium groups and, importantly, a strong electron-withdrawing group in *para*- or *ortho*-position to the leaving group. So far 4-[^{18}F]FTrp remains the only radiolabeled tryptophan analog prepared by using isotopic exchange supported by electron-withdrawing groups in the suitable position (Fig. 12).[131] The appropriate precursor containing a carbonyl group in 5 position for radiofluorination was obtained in 8% yield over 10 steps using Z-(*R*)-BMI [132] as a chiral glycine equivalent. The introduced carbonyl group as well as the N_{in}-Boc group activate the otherwise very electron rich indole system to enable nucleophilic aromatic ^{18}F/^{19}F exchange which was carried out using [^{18}F]TBAF in *N*,*N*-dimethylformamide (DMF) under microwave heating. The reaction mixture was irradiated with 50 W microwaves during 1 min affording the radiolabeled intermediate in RCY of up to 49%. The latter was reductively decarbonylated using the Wilkinson catalyst ($Rh(PPh_3)_3Cl$) in benzonitrile. Again, the application of microwaves instead of conventional heating, improved the yield of this step up to 75% and significantly reduced reaction time. Finally, deprotection using 12 M HCl at 150 °C for 30 min followed by HPLC purification furnished enantiomerically pure (*ee* > 99%) 4-[^{18}F]FTrp in a RCY of 13% within 100 min.

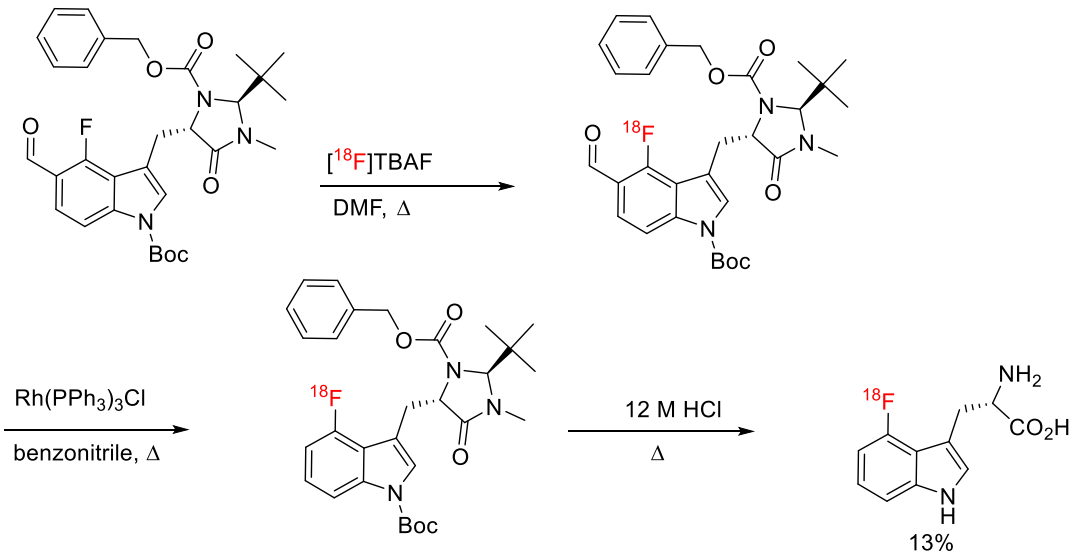

Figure 12: Preparation of 4-[^{18}F]FTrp using isotopic exchange.

3.4. Preparation of radiofluorinated tryptophans via Cu-mediated aromatic ^{18}F-fluorination and their preclinical evaluation

As already mentioned, the extremely electron rich nature of the indole ring impedes the preparation of fluorotryptophans labeled in aromatic positions using conventional radiofluorination protocols. This problem may be solved by the application of transition metal mediated aromatic ^{18}F-fluorination. This "Umpolung" approach discovered by Lee et al. (Fig. 13A)[133] allowed the introduction of ^{18}F into (hetero)arenes regardless of their electronic properties. The original protocol of Lee et al. comprises the reaction of a radiofluorinated Pd^{IV} complex prepared in advance with an appropriate Pd^{II}–aryl compound, yielding the corresponding ^{18}F-labeled arene after reductive elimination. A further development of this method involves radiolabeling of an arylnickel(II) complex with a radiofluorination agent generated *in situ* from a hypervalent iodine oxidant [bis(onio)-substituted aryliodine(III)] and [^{18}F]fluoride (Fig. 13B).[134-136] This protocol was successfully used to prepare *N*-Boc protected 5-[^{18}F]fluoroindole in 55% RCY. Unfortunately, Ni-mediated radiofluorination is hardly amenable to automated synthesis modules due to the high moisture sensitivity of the hypervalent iodine oxidant. This disadvantage has precluded so far the application of this procedure for the preparation of ^{18}F-labeled Trps.

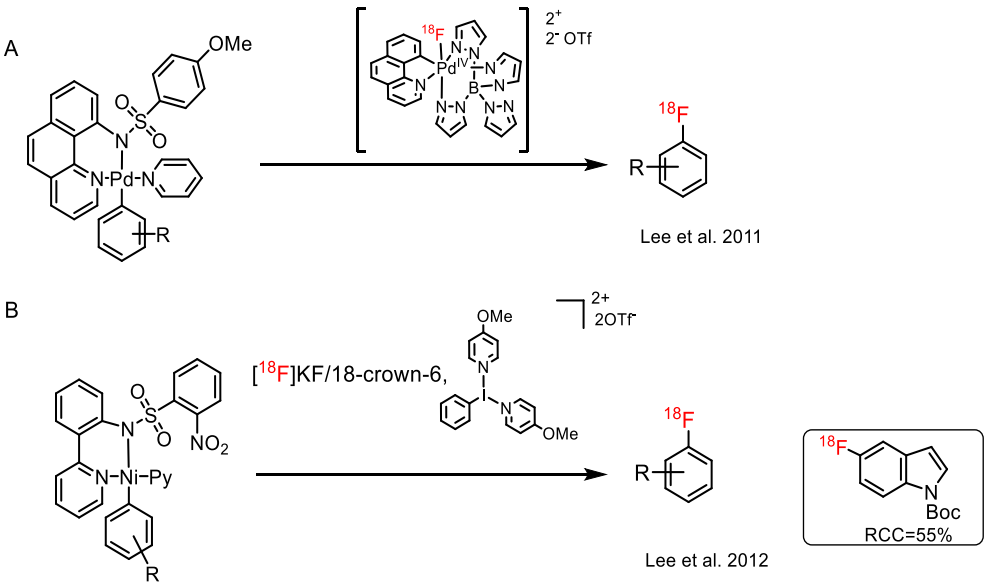

Figure 13. Pd- and Ni-mediated synthesis of [^{18}F]fluoro(hetero)arenes according to Lee *et al.* [133, 134]

In contrast, Cu-mediated aromatic ^{18}F-labeling pioneered by Ichiishi et al.[137] for (aryl)(mesityl)iodonium salts and later applied to aryl pinacol boronates (ArBPin),[138] aryl boronic acids,[139] aryl trialkyl stannanes,[140] and for directed CH-^{18}F-fluorination [141] features a simple reaction setup and does not utilize extremely sensitive, low stable and/or hardly accessible starting materials and reagents. No special precautions are necessary and reactions are carried out under air or argon. Commercially available $Cu(MeCN)_4OTf$, $Cu(Py)_4(OTf)_2$ and $Cu(OTf)_2$ are used as Cu-sources. Importantly, as well as Ni- and Pd-mediated radiofluorinations, Cu-mediated radiolabeling enables high-yielding preparation of ^{18}F-labeled electron-rich (hetero)aromatics and is, therefore, well suitable for the preparation of radiofluorinated tryptophan analogs. Unfortunately, though efficient in small-scale experiments, the original procedures were not well suited for PET tracer production on a practical scale. The reason for the failure was elucidated and led to the development novel radiolabeling procedures .[142]

$Cu(OTf)_2(py)_4$ and $Cu(MeCN)_4OTf$, typically applied as mediators, were found to be unstable under strong basic conditions conventionally applied to radiofluorinations (typically, 2.8–3.5 mg K_2CO_3 and 15 mg K2.2.2 or 18-crown-6; “high base” conditions). Consequently, under “high base” conditions, one-pot radiosynthesis provided radiofluorinated arenes best in 5–7% RCYs. In contrast, “low base” conditions (e. g.,

application of < 0.5 mg K_2CO_3 or low amounts of less basic Et_4NHCO_3) afforded ^{18}F-labeled model compounds in 41–64% RCYs.

The "low base" procedure was utilized for the preparation of 6-[^{18}F]FTrp. The application of methanolic Et_4NHCO_3 for the elution of [^{18}F]F$^-$ according to the "minimalist" approach (Richarz *et al.* 2014)[143] allowed to prepare ^{18}F-labeled 6-fluoroindolylmethyl substituted Schöllkopf's bis-lactim ether in 53% radiochemical conversion (RCC) (Fig. 14).[144] The subsequent hydrolysis with 50% H_2SO_4 followed by HPLC purification afforded the desired radiolabeled amino acid in 16% RCY within 110 min.

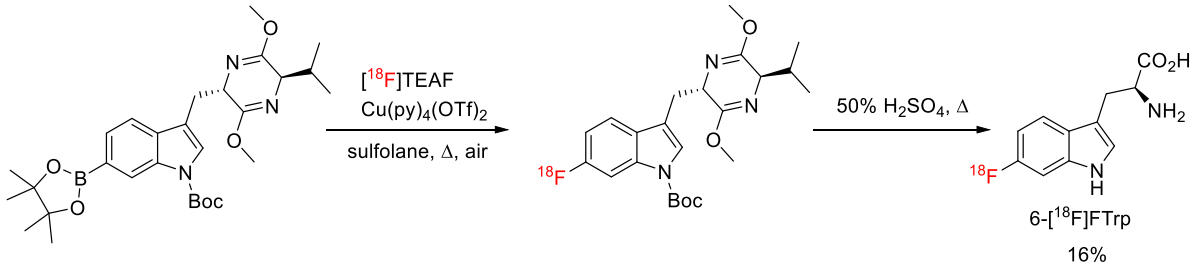

Figure 14. Synthesis of 6-[^{18}F]FTrp via Cu-mediated radiofluorination.

During following attempts to refine the Cu-mediated radiofluorination of boronic substrates it was serendipitously found that the application of primary and secondary alcohols as reaction co-solvents substantially increased ^{18}F-incorporation rates.[145] In the presence of *n*BuOH, highly electron rich unprotected 4-, 5-, and 6-indole boronic acids and pinacol boronates underwent near-quantitative (>96 %) radiofluorination. The applicability of the novel method to produce radiofluorinated Trps was confirmed by the preparation of protected radiolabeled 4- and 6-fluorotryptophans in RCCs of 92 and 99 %, respectively.

Preparation of 4–7-[^{18}F]FTrps via Cu-mediated radiofluorination and their biological evaluation

The alcohol-enhanced Cu-mediated radiofluorination was applied for the preparation of the hitherto unknown 7-[^{18}F]FTrp (Fig. 15, Table 1).[146] The corresponding boronate precursor, Boc-7-(Bpin)Trp-O*t*Bu, easily accessible from Boc-Trp-O*t*Bu using a one pot two step sequence comprised Ir-catalyzed 2,7-diborylation followed by the regioselective 2-protodeborylation,[147] was radiolabeled in *n*BuOH/*N*,*N*-

dimethylacetamide (DMA) furnishing intermediate Boc-7-[^{18}F]FTrp-O*t*Bu in >90% RCC. The latter was deprotected using 38% HCl/MeOH affording, after HPLC purification, the desired PET probe in 41% RCY within 100–110 min. Similarly, 4–6-[^{18}F]FTrps were produced from the corresponding Boc-n-(Bpin)Trp-O*t*Bu precursors (n = 4–6) in RCYs of 40–53% (Table 1). In all cases, enantiomeric purities (*ee*) exceeded 99% and the Cu content in the final solutions was below any level of concern.

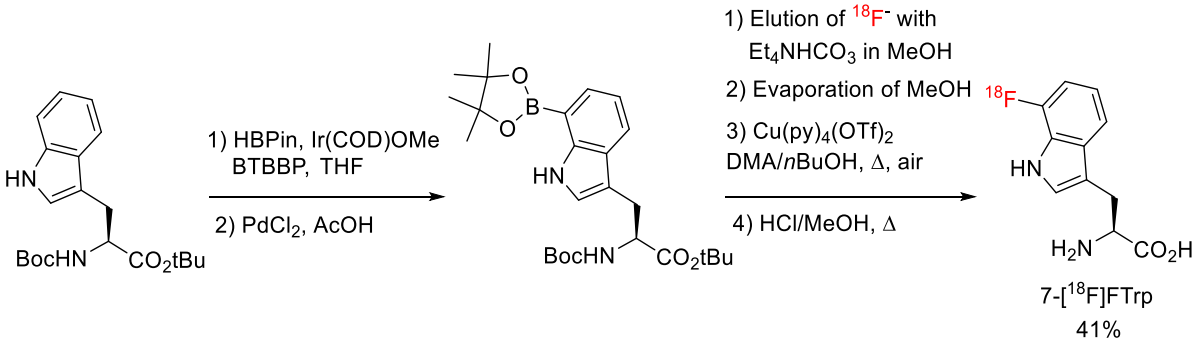

Figure 15. Preparation of 4–7-[^{18}F]FTrp via alcohol-enhanced Cu-mediated radiofluorination.

Tang *et al*. prepared (*R*)- and (*S*)-5-[^{18}F]FTrps in 1.5±0.6% RCY within 193±46 min via Cu-mediated radiolabeling of the racemic precursor using DMF as reaction solvent and K2.2.2/K_2CO_3 as a base followed by deprotection of the radiolabeled Boc-(*RS*)-5-[^{18}F]FTrp and separation of enantiomers.[148] Giglio et al. synthesized 4-(*RS*)-[^{18}F]FTrp, 5-[^{18}F]FTrp, 6-[^{18}F]FTrp, and 7-(*RS*)-[^{18}F]FTrp via Cu-mediated [^{18}F]fluorination in DMF/MeCN using Bu_4NHCO_3 as a base in RCYs of 4–12%.[149] 5-7-[^{18}F]FTrps were also produced in 15–24% RCYs using Cu-mediated radiofluorination under “low base” conditions (Table 1).[138, 144]

Taken together, synthesis of 5- and 6-[^{18}F]FTrps applying the Balz-Schiemann reaction is interesting only from the historical point of view. The application of ^{18}F/^{19}F isotopic exchange using a transient activating group for the production of [^{18}F]FTrps is less attractive than Cu-mediated ^{18}F-fluorination of suitably protected Bpin-substituted tryptophans by means of the precursor accessibility as well as simplicity and efficacy of the radiosynthesis procedure. If the latter approach was used, application of Boc and *t*Bu protecting groups for amino and carboxylic groups, respectively, enabled smooth and fast deprotection of radiolabeled intermediates under rather mild acidic conditions. Double protection of the amino group as well as protection of the indole nitrogen was

unnecessary and in some cases even deleterious. Furthermore, the literature data, summarized in Table 1, underline the superiority of alcohol-enhanced Cu-mediated radiofluorination over other protocols used for the preparation of [^{18}F]FTrps. This method enabled synthesis of four regioisomeric radiolabeled tryptophans with RCYs significantly higher within the same preparation time or even faster than other published protocols.

Table 1. Comparison of the different procedures for the preparation of [^{18}F]FTrps

	Zlatopolskiy *et al.*[146]	Atkins *et al.*[130]	Weiss *et al.*[131]	"Low base"[144]	Giglio *et al.*[149]	Tang *et al.*[148]
n-[^{18}F]FTrp (RCY, %)	4- (40±12) 5- (53±5) 6- (30±3)[a] 6- (42±5)[b,c] 7- (41±3)	5- (9–10)[c] 6- (9–10)[c]	4- (13)	5- (23±8) 6-(15±4)[a,d] 7- (24±5)[d]	4- (8)[c,e] 5- (12) 6- (4)[e] 7- (9)[c,e]	5-: (1.5%)
Synthesis time (min)	100–110	255	115	100–110	n. d.	193
ee	>99; 89[a]	–	>99	>99; 89[a]	n. d.	73–82,[f,g] 98[g,h]
Molar activity (GBq/µmol)	95–240	5×10^{-4}	7×10^{-7}	95–240	n. d.	403–722

a: from bis-lactime precursor; b: from Boc-6-BpinTrp-OtBu; c: racemic; d:[146]; e: estimated by the separation of a small portion of the reaction mixture; f: 5-(S)-[^{18}F]FTrp; g: after separation of the racemic mixture by preparative enantioselective HPLC; h: 5-(R)-[^{18}F]FTrp; n.d.: no data. Reproduced with permission from.[146]

Zlatopolskiy *et al*. studied 4–7-[^{18}F]FTrps in seven different tumor cell lines and compared them to *O*-(2-[^{18}F]fluoroethyl)tyrosine ([^{18}F]FET) (Fig. 16).[146] The latter PET tracer is commonly used for the visualization of amino acid transporters and, indirectly, of the protein synthesis especially in brain tumors.[150] [^{18}F]FET and [^{18}F]FTrps are aromatic amino acids which are transported into cells mainly by L-amino acid transporters predominantly of type 1 (LAT1). [^{18}F]FET protein incorporation rate is very low. This tracer is intracellularly trapped presumably owing to the asymmetry of the intra- and extracellular recognition by LAT1.[151] Cellular accumulation of [^{18}F]FET and [^{18}F]FTrps was studied, i.a., in MDA-MB-231 and MCF-7 breast tumor cell lines.[146] The low expression of IDO1 in MDA-MB-231 cells can be stimulated by the incubation with interferon-γ (γITF) in a time-dependent manner. LAT1 expression is not induced by γITF.[152] Expression of IDOs in MCF7 cells remains very low even under γITF stimulation.[153] In contrast, these cells express an increased level of TPH1.[154] While there were no substantial differences in accumulation of [^{18}F]FTrps and [^{18}F]FET in untreated MDA-MB-231 cells, the uptake of 6- and 7-[^{18}F]Trps significantly increased after γITF stimulation (up to 2× and 7× after 1 and 2 h incubation, respectively, Fig. 13). [^{18}F]FET uptake was only slightly altered after γITF stimulation. Uptake in MCF7 cells was about 2 times higher for 7-[^{18}F]FTrp than for [^{18}F]FET. Protein incorporation of 7-[^{18}F]FTrp measured in three tumor cell lines was insignificant and amounted to 2–3% of the cellular accumulated radioactivity.

Tang et al. studied uptake of 5-(*S*)- and 5-(*R*)-[^{18}F]FTrps in CT26, CT26-hIDO1 and CT26-hTDO2 cells with and without doxycycline-induced overexpression of hIDO1 and hTDO2 [148]. This study revealed that only the (*S*)-isomer was more efficiently trapped in cells upon induction of IDO1 and TDO2 enzymes compared to the corresponding control groups treated with sucrose. The elevated cellular uptake of the (*R*)-isomer was not observed.

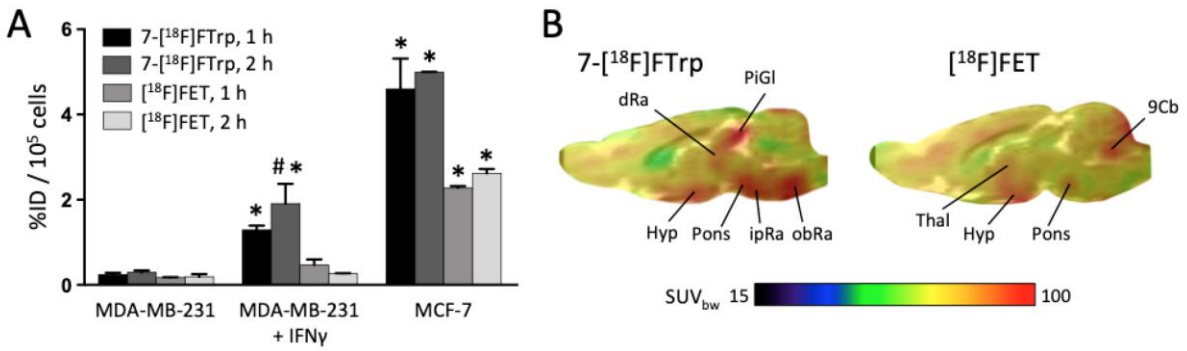

Figure 16. Comparison of *in vitro* cell uptake and *in vivo* brain distribution of 7-[^{18}F]FTrp and [^{18}F]FET. A: Tracer uptake in breast cancer MDA-MB-231 (with and without INFγ) and MCF-7 cells (n=3 each). B: Tracer uptake in the brain of healthy rats, 90–120 min post injection (mean images, n=3 each). # Significantly different from 1 h. $F(1,24)=5.9$, $p=0.0234$ for factor time, posthoc $p<0.05$. * Significantly different from all others at the same time point. $F(5,24)=307.3$, $p<0.0001$ for factor tracer/cell line, posthoc $p<0.05$. Abbreviations: 9Cb: cerebellar lobule 9, dRa: dorsal raphe, Hyp: hypothalamus, ipRa: raphe interpositus, obRa: raphe obscurus, PiGl: pineal gland, Thal: thalamus.

Brain distribution of 4–7-[^{18}F]FTrps was evaluated in healthy rats.[146] For 4–6-[^{18}F]FTrps rapidly *in vivo* defluorination was observed reflected by high radioactivity accumulation in the skull. Similarly, Tang et al. observed fast defluorination of 5-[^{18}F]FTrp in tumor bearing immunocompromised mice.[148] In contrast to the other radiofluorinated tryptophans, 7-[^{18}F]FTrp demonstrated a high *in vivo* stability clearly reflected by low skull uptake. Furthermore, accumulation of 7-[^{18}F]FTrp was observed in serotonergic areas like dorsal raphe and hypothalamus as well as melatonin-producing pineal gland (Fig. 15). This brain biodistribution pattern was markedly different from [^{18}F]FET. The latter accumulated mainly in areas with high protein/peptide hormone synthesis rate like thalamus, hypothalamus, cerebellum, and pons.

The pronounced *in vivo* instability of 4–6-[^{18}F]FTrps and conversely the observed *in vivo* stability of 7-[^{18}F]FTrp could be well explained by the substrate specificity of IDO and TDO taking into account that the kynurenine pathway accounts for at least 95% of the catabolism of Trp. Indeed, 6-FTrp is the best known substrate of TDO with V_{max}/K_m approximately 1.6-fold higher than that of Trp.[155] 5-FTrp is also a relatively good

substrate of TDO with a V_{max}/K_m value of about 70% relative to that of native tryptophan. In contrast, 4-FTrp is no substrate of TDO. However, this amino acid as well as 5- and 6-FTrps is metabolized by IDO with a V_{max}/K_m value of 14, 37 and 47% to that of Trp, respectively.[156] Notably, 7-FTrp is no substrate of either TDO or IDO but, instead, an inhibitor of both enzymes. Tang et al. observed a noticeably slower defluorination of 5-[^{18}F]FTrp in TDO knock-out ($TDO^{-/-}$) compared to wild type mice.[148] These data support the involvement of TDO in the defluorination process.

The potential of 7-[^{18}F]FTrp for tumor imaging was evaluated in MCF-7, PC-3 and NCI-H69 xenografts in the chicken chorioallantoic membrane (CAM) model.[157] 7-[^{18}F]FTrp and, for comparison, $^{18}F^-$ were administered (Fig. 17). The $^{18}F^-$ PET scans performed after 30 min p.i. displayed tracer uptake mainly in bones, joints and beak of the chicken embryos. No significant tumor accumulation was observed. In contrast, 7-[^{18}F]FTrp PET clearly delineated the tumors.

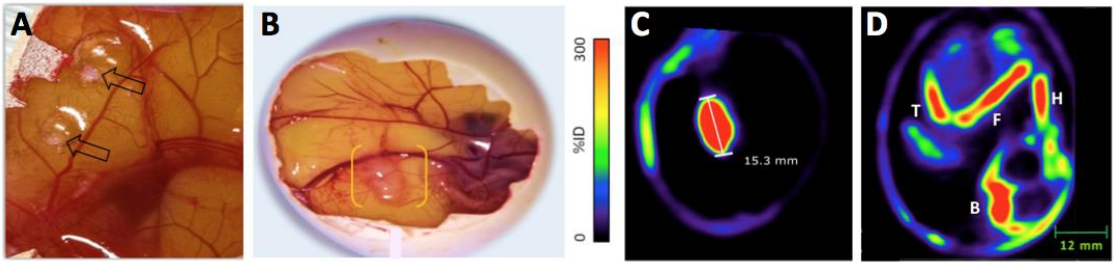

Figure 17. MCF7 CAM xenograft A: Chorioallantoic membrane with inoculated tumor clusters (arrows) 30 min after implantation. B: MCF7 CAM xenograft 7 days after implantation. C: 7-[^{18}F]FTrp uptake in a MCF7 tumor. D: Biodistribution of $^{18}F^-$ in a chicken embryo (B: beak; F: femur; H: humerus; T: tibia).

Preparation and preliminary biological evaluation of 5-[^{18}F]fluoro-α-methyltryptophan (5-[^{18}F]F-AMT)

5-[^{18}F]F-AMT was produced via Cu-mediated radiofluorination of two different Bpin precursors (Fig. 18).[149] In both cases radiolabeling was carried out in DMF/MeCN using [^{18}F]TBAF and $Cu(Py)_4(OTf)_2$ at 110 °C for 20 min. Labeling of the more easily accessible (*S*)-2-methyl-8-(phenylsulfonyl)-5-(4,4,5,5-tetramethyl-1,3,2-dioxaborolan-2-yl)-3,8-dihydropyrrolo[2,3-b]indole-1,2(2*H*)-dicarboxylate (Fig. 18A) followed by

deprotection of the radiofluorinated intermediate with TFA and KOH afforded the desired tracer in 11% RCY (starting from azeotropically dried [^{18}F]TBAF). Alternatively, ^{18}F-fluorination of *tert*-butyl (*S*)-3-(2-[(*tert*-butoxycarbonyl)amino]-3-methoxy-2-methyl-3-oxopropyl)-5-(4,4,5,5-tetramethyl-1,3,2-dioxaborolan-2-yl)-1*H*-indole-1-carboxylate followed by a two-step deprotection delivered 5-[^{18}F]F-AMT in a higher RCY of 15% (Fig. 18B).

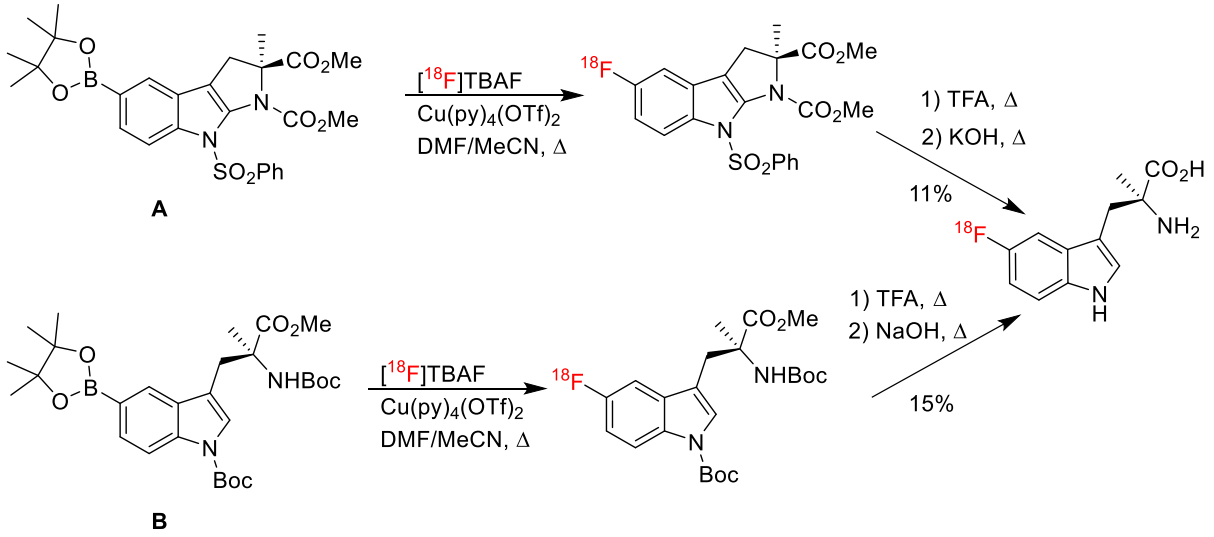

Figure 18. Preparation of 5-[^{18}F]F-AMT from two different precursors.

Cellular uptake of 5-[^{18}F]F-AMT in γITF-stimulated HeLa tumor cells was significantly higher than in untreated cells [3.5±0.6% vs. 0.5±0.3% after 1 h incubation ($p<0.001$)] and significantly inhibited by NLG919, a known IDO1 inhibitor, indicating dependence of 5-[^{18}F]F-AMT cellular uptake on IDO1 expression. 5-[^{18}F]F-AMT PET imaging revealed tracer accumulation in IDO-1 positive B16F10 tumor xenografts in immunocompromised mice.[149]

3.5 **Preparation and preliminary *in vitro* characterization of 2-[^{18}F]trifluoromethyltryptophan (2-[^{18}F]CF_3-Trp)**

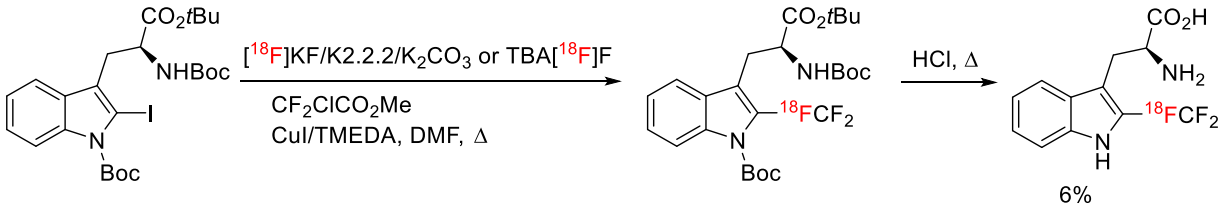

Figure 19. Synthesis of 2-[^{18}F]CF_3-Trp.

Kim et al. [158] prepared 2-[^{18}F]CF_3-Trp using a modified arene trifluoromethylation procedure described by Su et al. [159] transferred to radiosynthesis. Accordingly, Boc-2-ITrp-O*t*Bu was treated with [^{18}F]KF/K2.2.2/K_2CO_3 or [^{18}F]TBAF and methyl chlorodifluoroacetate in the presence of CuI/*N*,*N*,*N*′,*N*′-tetramethylethylendiamine (TMEDA) in DMF at 150 °C for 15 min to give Boc-2-[^{18}F]CF_3-Trp-O*t*Bu in RCYs of up to 56% (Fig. 19). Deprotection was performed by 1 M HCl at 110 °C for 10 min furnishing the desired tracer in a RCY of 6±2% within 70 min in excellent radiochemical and enantiomeric purities and with an acceptable molar activity of 0.44–0.76 GBq/µmol (1.5–4 GBq tracer). 2-[^{18}F]CF_3-Trp was completely stable in human or mouse serum at least for 6 h and demonstrated low binding to serum proteins. Metabolism of 2-CF_3-Trp in BALB/c mice studied by LC/MS demonstrated fast metabolism of the Trp analog in brain and blood furnishing mainly 2-CF_3-serotonine/2-CF_3-tryptamine and 2-CF_3-serotonine, respectively. In contrast, only unchanged 2-CF_3-Trp was found in urine.

4. Relationships between the structure of tryptophan analogs and their suitability as PET-tracers

In this chapter, we briefly summarize some relationships between the structure of tryptophan analogs and their pharmacological properties, which could be helpful for the development of novel PET-tracers.

1) Radiolabeled 5-OHTrp analogs could be used for visualization of serotonergic tissues. However, unspecific uptake in dopaminergic and noradrenergic areas owing to the high affinity to AADC as well as some metabolization via the KYN pathway should be taken into account.
2) [Carboxy-^{11}C]tryptophans can not be used for the visualization of Trp metabolism.

3) α-Methyl substituted serotonins are not degraded by monoamine oxidase and trapped in serotonergic areas.
4) α-Methyltryptophans are no substrates for IDO. However, they are, presumably, substrates for tryptophan selective transporters, which are upregulated by the activation of the KYN pathway.
5) α-Methyltryptamines, the products of decarboxylation of AMTs by AADC, are inhibitors of monoamine oxidase A.
6) Trp analogs containing bulky [^{18}F]fluoroalkoxy or [^{18}F]fluoroalkyl (and, presumably, alkoxy and alkyl) substituents at the 2–7 positions of the indole ring are not able to target Trp metabolism. Instead, they are substrates for LAT1 amino acid transporters.
7) 2-[^{18}F]CF_3Trp is, presumably, able to target the serotonin biosynthesis but not the KYN metabolism.
8) 1-[^{18}F]FETrp and 1-[^{11}C]MeTrp are substrates for IDO but not for TPH.
9) Uptake of 1-[^{18}F]FETrp in tumor cells is partially dependent on IDO expression.
10) 4–6-[^{18}F]FTrps are not stable *in vivo*.
11) In contrast, 7-[^{18}F]FTrp is stable *in vivo*, and accumulates in serotonergic areas and the melatonin-producing pineal gland in rat brains. 7-[^{18}F]FTrp uptake in tumor cells depends on IDO expression.
12) 5-^{18}F-Labeled Trps could be used for the visualization of serotonin biosynthesis only if they are inhibitors of TPH.

5. Conclusion

Dysregulation of tryptophan metabolic pathways represents a prominent hallmark of various pathologies. Several ^{11}C-labeled tryptophans, and especially α-[^{11}C]methyltryptophan ([^{11}C]AMT) have already demonstrated their potential for tumor- and neuro-diagnostics. However, the short half-life of ^{11}C and laborious preparation of these radiotracers prevent their broader clinical application. The rapid development of radiolabeling methods in the last decade and, first of all, the discovery of Cu-mediated ^{18}F-fluorination enabled efficient preparation of radiofluorinated Trp analogs which were hardly or even not accessible before in amounts sufficient for their

preclinical and clinical evaluation. In particular, 5-[^{18}F]fluoro-α-methyltryptophan (5-[^{18}F]F-AMT), 1-(2-[^{18}F]fluoroethyl)tryptophan (1-[^{18}F]FETrp) and 7-[^{18}F]fluorotryptophan (7-[^{18}F]FTrp), already demonstrated their potential in preclinical studies, are promising candidates which might improve clinical diagnostics of age-associated disorders in the near future.

6. Acknowledgements

This work was supported by the DFG grants ZL 65/1-1, ZL 65/3-1, EN 439/6-1 and Russian foundation of basic researches, grant 20-53-12030\20, joint project with DFG ZL 65/4-1.

7. References

1. M. L. Orr, B. K. Watt. *Amino acid content of foods*, United States Department of Agriculture, U.S. Govt. Print. Off., Washington, D.C., 1957
2. V. Selvaraj, D. M. Stocco. *Trends Endocrinol. Metab.,* **26**, 341 (2015)
3. D. M. Richard, M. A. Dawes, C. W. Mathias, A. Acheson, N. Hill-Kapturczak, D. M. Dougherty. *Int. J. Tryptophan. Res.*, **2**, 45 (2009)
4. O. Takikawa. *Biochem. Biophys. Res. Commun.*, **338**, 12 (2005)
5. C. R. MacKenzie, K. Heseler, A. Muller, D. Walter. *Curr. Drug Metab.*, **8**, 237 (2007)
6. S. A. Rafice, N. Chauhan, I. Efimov, J. Basran, E. L. Raven. *Biochem. Soc. Trans.*, **37**, 408 (2009)
7. A. W. S. Yeung, A. C. Terentis, N. J. C. King, S. R. Thomas. *Clin. Sci.,* **129**, 601 (2015)
8. M. Kanai, H. Funakoshi, H. Takahashi, T. Hayakawa, S. Mizuno, K. Matsumoto, T. Nakamura. *Mol Brain,* **2**, 8 (2009)
9. A. A.-B. Badawy. *Int. J. Tryptophan Res.*, **10**, 1178646917691938 (2017)
10. K. Swartz, M. During, A. Freese, M. Beal. *J. Neurosci.*, **10**, 2965 (1990)
11. E. Kwidzinski, I. Bechmann. *J. Mol. Med.,* **85**, 1351 (2007)
12. R. Schwarcz, J. P. Bruno, P. J. Muchowski, H.-Q. Wu. *Nat Rev Neurosci,* **13**, 465 (2012)
13. A. Vescia, G. di Prisco. *J. Biol. Chem.,* **237**, 2318 (1962)
14. G. J. Guillemin, K. M. Cullen, C. K. Lim, G. A. Smythe, B. Garner, V. Kapoor, O. Takikawa, B. J. Brew. *J. Neurosci.,* **27**, 12884 (2007)
15. B. Olivier. *Eur. J. Pharmacol.,* **753**, 2 (2015)
16. S. Banskota, J.-E. Ghia, W. I. Khan. *Biochimie,* **161**, 56 (2019)
17. C. Maximino. *Serotonin and Anxiety, Neuroanatomical, Pharmacological, and Functional Aspects*, Springer-Verlag, New York, 2012
18. S. Vancassel, L. Capuron, N. Castanon. *Front. Neurosci.,* **12**, (2018)

19. S. Tordjman, S. Chokron, R. Delorme, A. Charrier, E. Bellissant, N. Jaafari, C. Fougerou. *Curr. Neuropharmacol.,* **15**, 434 (2017)
20. R. Hardeland, D. P. Cardinali, V. Srinivasan, D. W. Spence, G. M. Brown, S. R. Pandi-Perumal. *Prog. Neurobiol.,* **93**, 350 (2011)
21. R. Hardeland. *Aging Dis,* **3**, 194 (2012)
22. D. C. Maddison, F. Giorgini. *Semin. Cell Dev. Biol.,* **40**, 134 (2015)
23. M. Politis, F. Niccolini. *Behav. Brain Res.,* **277**, 136 (2015)
24. J. J. Rodríguez, H. N. Noristani, A. Verkhratsky. *Prog. Neurobiol.,* **99**, 15 (2012)
25. A. C. Rubin de Celis Ferrari, J. Glasberg, R. P. Riechelmann. *Clinics,* **73**, e490s (2018)
26. M. Zamanakou, A. E. Germenis, V. Karanikas. *Immunol. Lett.,* **111**, 69 (2007)
27. S. Geisler, P. Mayersbach, B. Kathrin, H. Schennach, D. Fuchs, J. M. Gostner. *Pteridines,* **26**, 31 (2015)
28. A. A.-B. Badawy, G. Guillemin. *Int. J. Tryptophan Res.,* **12**, 1178646919868978 (2019)
29. H. Orlefors, A. Sundin, U. Garske, C. Juhlin, K. Oberg, B. Skogseid, B. Långström, M. Bergstrom, B. Eriksson. *J. Clin. Endocrinol. Metab.,* **90**, 3392 (2005)
30. D. C. Chugani, O. Muzik. *J. Cereb. Blood Flow Metab.,* **20**, 2 (2000)
31. L. M. Paterson, B. R. Kornum, D. J. Nutt, V. W. Pike, G. M. Knudsen. *Med. Res. Rev.,* **33**, 54 (2013)
32. J. Zessin, J. Steinbach. *J. Labelled Compd. Radiopharm.,* **41**, 669 (1998)
33. H. T. Bucherer, W. Steiner. *J. prakt. Chem.,* **140**, 291 (1934)
34. L. C. Washburn, T. T. Sun, B. L. Byrd, R. L. Hayes, T. A. Butler. *J. Nucl. Med,* **20**, 857 (1979)
35. R. L. Hayes, L. C. Washburn, B. W. Wieland, T. T. Sun, J. B. Anon, T. A. Butler, A. P. Callahan. *Int. J. Appl. Radiat. Isot.,* **29**, 186 (1978)
36. R. L. Hayes, L. C. Washburn, B. W. Wieland, T. T. Sun, R. R. Turtle, T. A. Butler. *J. Nucl. Med,* **17**, 748 (1976)
37. M. R. Zalutsky, J. Wu, P. V. Harper, T. Wickland. *Int. J. Appl. Radiat. Isot.,* **32**, 182 (1981)
38. J. Ermert, H. H. Coenen. *J. Labelled Compd. Radiopharm.,* **56**, 225 (2013)
39. A. Popkov, P. H. Elsinga. *Curr. Org. Chem.,* **17**, 2127 (2013)
40. A. Pekošak, U. Filp, A. J. Poot, A. D. Windhorst. *Mol. Imaging Biol.,* **20**, 510 (2018)
41. E. S. da Silva, V. Gómez-Vallejo, Z. Baz, J. Llop, F. López-Gallego. *Chem. - Eur. J.,* **22**, 13619 (2016)
42. P. Bjurling, Y. Watanabe, M. Tokushige, T. Oda, B. Långström. *J. Chem. Soc., Perkin Trans. 1,* 1331 (1989)
43. O. Eriksson, R. Selvaraju, B. Borg, V. Asplund, S. Estrada, G. Antoni. *Nucl. Med. Biol.,* **40**, 567 (2013)
44. P. Bjurling, Y. Watanabe, B. Långström. *Appl. Rad. Isot.,* **39**, 627 (1988)
45. M. Ikemoto, M. Sasaki, T. Haradahira, T. Yada, H. Omura, Y. Furuya, Y. Watanabe, K. Suzuki. *Appl. Rad. Isot.,* **50**, 715 (1999)
46. M. Sasaki, M. Ikemoto, M. Mutoh, T. Haradahira, A. Tanaka, Y. Watanabe, K. Suzuki. *Appl. Rad. Isot.,* **52**, 199 (2000)
47. O. C. Neels, P. L. Jager, K. P. Koopmans, E. Eriks, E. G. E. de Vries, I. P. Kema, P. H. Elsinga. *J. Labelled Compd. Radiopharm.,* **49**, 889 (2006)
48. N. Harada, S. Nishiyama, K. Sato, H. Tsukada. *Appl. Rad. Isot.,* **52**, 845 (2000)
49. A. K. D. Visser, A. van Waarde, A. T. M. Willemsen, F. J. Bosker, P. G. M. Luiten, J. A. den Boer, I. P. Kema, R. A. J. O. Dierckx. *Eur. J. Nucl. Med. Mol. Imaging,* **38**, 576 (2011)

50. P. Hartvig, K. J. Lindner, J. Tedroff, Y. Andersson, P. Bjurling, B. Långström. *J. Neural Transm.: Gen. Sect.,* **88**, 1 (1992)
51. P. Lundquist, P. Hartvig, G. Blomquist, M. Hammarlund-Udenaes, B. Långström. *J. Cereb. Blood Flow Metab.,* **27**, 821 (2007)
52. F. Yamazaki, T. Kuroiwa, O. Takikawa, R. Kido. *Biochem. J.,* **230**, 635 (1985)
53. T. Furmark, I. Marteinsdottir, A. Frick, K. Heurling, M. Tillfors, L. Appel, G. Antoni, P. Hartvig, H. Fischer, B. Långström, E. Eriksson, M. Fredrikson. *J. Psychopharmacol.,* **30**, 1028 (2016)
54. O. Eriksson, A. Wall, I. Marteinsdottir, H. Ågren, P. Hartvig, G. Blomqvist, B. Långström, T. Naessén. *Psychiatry Res., Neuroimaging,* **146**, 107 (2006)
55. H. Ågren, L. Reibring, P. Hartvig, J. Tedroff, P. Bjurling, K. Hörnfeldt, Y. Andersson, H. Lundqvist, B. Långström. *Acta Psychiatr. Scand.,* **83**, 449 (1991)
56. O. Eriksson, D. Espes, R. K. Selvaraju, E. Jansson, G. Antoni, J. Sorensen, M. Lubberink, A. R. Biglarnia, J. W. Eriksson, A. Sundin, H. Ahlström, B. Eriksson, L. Johansson, P. O. Carlsson, O. Korsgren. *Diabetes,* **63**, 3428 (2014)
57. A. K. Visser, N. K. Ramakrishnan, A. T. Willemsen, V. Di Gialleonardo, E. F. de Vries, I. P. Kema, R. A. Dierckx, A. van Waarde. *J. Cereb. Blood Flow Metab.*, **34**, 118 (2014)
58. T. Brabander, D. J. Kwekkeboom, R. A. Feelders, A. H. Brouwers, J. J. Teunissen. *Front. Horm. Res.,* **44**, 73 (2015)
59. M. Fraenkel, A. Faggiano, G. D. Valk. *Front. Horm. Res.,* **44**, 1 (2015)
60. O. C. Neels, K. P. Koopmans, P. L. Jager, L. Vercauteren, A. Van Waarde, J. Doorduin, H. Timmer-Bosscha, A. H. Brouwers, E. G. E. De Vries, R. A. J. O. Dierckx, I. P. Kema, P. H. Elsinga. *Cancer Res.,* **68**, 7183 (2008)
61. K. P. Koopmans, O. C. Neels, I. P. Kema, P. H. Elsinga, W. J. Sluiter, K. Vanghillewe, A. H. Brouwers, P. L. Jager, E. G. E. De Vries. *J. Clin. Oncol.,* **26**, 1489 (2008)
62. P. Bjurling, G. Antoni, Y. Watanabe, B. Långström. *Acta Chem. Scand.,* **44**, 178 (1990)
63. A. Sundin, B. Eriksson, M. Bergström, P. Bjurling, K.-J. Lindner, K. Öberg, B. Långström. *Nucl. Med. Biol.,* **27**, 33 (2000)
64. X. Shao, R. Hoareau, A. C. Runkle, L. J. M. Tluczek, B. G. Hockley, B. D. Henderson, P. J. H. Scott. *J. Labelled Compd. Radiopharm.,* **54**, 819 (2011)
65. D. Comar, M. Maziere, C. Crouzel, in *International Atomic Energy Agency (IAEA),* 1973, pp. 461
66. M. Holschbach, M. Schüller. *Appl. Rad. Isot.,* **44**, 779 (1993)
67. J. M. Link, K. A. Krohn, J. C. Clark. *Nucl. Med. Biol.,* **24**, 93 (1997)
68. P. Larsen, J. Ulin, K. Dahlstrøm, M. Jensen. *Appl. Rad. Isot.,* **48**, 153 (1997)
69. T. Chaly, M. Diksic. *J. Nucl. Med,* **29**, 370 (1988)
70. M. Suehiro, H. T. Ravert, A. A. Wilson, U. Scheffel, R. F. Dannals, H. N. Wagner. *J. Labelled Compd. Radiopharm.,* **31**, 151 (1992)
71. S. Mzengeza, T. K. Venkatachalam, M. Diksic. *Nucl. Med. Biol.,* **22**, 303 (1995)
72. A. Plenevaux, C. Lemaire, G. Delfiore, D. Comar. *Appl. Rad. Isot.,* **45**, 651 (1994)
73. P. K. Chakraborty, T. J. Mangner, D. C. Chugani, O. Muzik, H. T. Chugani. *Nucl. Med. Biol.,* **23**, 1005 (1996)
74. X. Huang, X. Xiao, R. J. Gillies, H. Tian. *Nucl. Med. Biol.,* **43**, 303 (2016)
75. P. Nordeman, U. Yngve, H. Wilking, S. Å. Gustavsson, J. Eriksson, G. Antoni. *J. Labelled Compd. Radiopharm.,* **61**, 1106 (2018)
76. M. Diksic, S. Nagahiro, T. L. Sourkes, Y. L. Yamamoto. *J. Cereb. Blood Flow Metab.,* **10**, 1 (1990)

77. B. K. Madras, T. L. Sourkes. *Biochem. Pharmacol.*, **14**, 1499 (1965)
78. P. Rosa-Neto, M. Diksic, M. Leyton, S. Mzengeza, C. Benkelfat. *Eur. J. Nucl. Med. Mol. Imaging*, **32**, 1199 (2005)
79. M. Diksic. *J Psychiatry Neurosci*, **26**, 293 (2001)
80. M. E. Greig, R. A. Walk, A. J. Gibbons. *J. Pharmacol. Exp. Ther.*, **127**, 110 (1959)
81. J. Tong, J. H. Meyer, Y. Furukawa, I. Boileau, L.-J. Chang, A. A. Wilson, S. Houle, S. J. Kish. *J. Cereb. Blood Flow Metab.*, **33**, 863 (2013)
82. E. Perreau-Linck, M. Beauregard, P. Gravel, V. Paquette, J. P. Soucy, M. Diksic, C. Benkelfat. *J. Psychiatry. Neurosci.*, **32**, 430 (2007)
83. A. Berney, M. Nishikawa, C. Benkelfat, G. Debonnel, G. Gobbi, M. Diksic. *Neurochem. Int.*, **52**, 701 (2008)
84. B. N. Frey, I. Skelin, Y. Sakai, M. Nishikawa, M. Diksic. *Psychiatry Res., Neuroimaging*, **183**, 157 (2010)
85. A. Berney, M. Leyton, P. Gravel, I. Sibon, D. Sookman, P. R. Neto, M. Diksic, A. Nakai, G. Pinard, C. Todorov, H. Okazawa, P. Blier, T. E. Nordahl, C. Benkelfat. *Arch. Gen. Psychiatry*, **68**, 732 (2011)
86. J. I. Lissemore, D. Sookman, P. Gravel, A. Berney, A. Barsoum, M. Diksic, T. E. Nordahl, G. Pinard, I. Sibon, J. Cottraux, M. Leyton, C. Benkelfat. *Transl. Psychiatry*, **8**, (2018)
87. M. Behen, H. T. Chugani, C. Juhász, E. Helder, A. Ho, M. Maqbool, R. D. Rothermel, J. Perry, O. Muzik. *Mov. Disord.*, **22**, 2256 (2007)
88. L. Booij, J. P. Soucy, S. N. Young, M. Regoli, P. Gravel, M. Diksic, M. Leyton, R. O. Pihl, C. Benkelfat. *J. Neurochem.*, **131**, 634 (2014)
89. Y. Sakai, M. Nishikawa, M. Diksic, M. Aubé. *Cephalalgia*, **34**, 165 (2013)
90. D. C. Chugani. *Biomarkers Med.*, **5**, 567 (2011)
91. S. Bagla, D. Cukovic, E. Asano, S. Sood, A. Luat, H. T. Chugani, D. C. Chugani, A. A. Dombkowski. *Neurobiol Dis*, **109**, 76 (2018)
92. E. Bosnyák, D. O. Kamson, A. R. Guastella, K. Varadarajan, N. L. Robinette, W. J. Kupsky, O. Muzik, S. K. Michelhaugh, S. Mittal, C. Juhász. *Neuro-oncology*, **17**, 1284 (2015)
93. J.-W. Jeong, C. Juhász, S. Mittal, E. Bosnyák, D. O. Kamson, G. R. Barger, N. L. Robinette, W. J. Kupsky, D. C. Chugani. *Cancer Imaging*, **15**, 10 (2015)
94. C. Juhász, O. Muzik, D. C. Chugani, H. T. Chugani, S. Sood, P. K. Chakraborty, G. R. Barger, S. Mittal. *J. Neuro-Oncol.*, **102**, 409 (2011)
95. F. John, E. Bosnyák, N. L. Robinette, A. J. Amit-Yousif, G. R. Barger, K. D. Shah, S. K. Michelhaugh, N. V. Klinger, S. Mittal, C. Juhász. *Neuro-Oncology*, **21**, 264 (2018)
96. J. Henrottin, A. Zervosen, C. Lemaire, F. Sapunaric, S. Laurent, B. Van den Eynde, S. Goldman, A. Plenevaux, A. Luxen. *ACS Med. Chem. Lett.*, **6**, 260 (2015)
97. J. D. Silk, S. Lakhal, R. Laynes, L. Vallius, I. Karydis, C. Marcea, C. A. R. Boyd, V. Cerundolo. *J. Immunol.*, 1000815 (2011)
98. D. E. Lyon, J. M. Walter, A. R. Starkweather, C. M. Schubert, N. L. McCain. *BMC Res. Notes*, **4**, 156 (2011)
99. C. Juhász, Z. Nahleh, I. Zitron, D. C. Chugani, M. Z. Janabi, S. Bandyopadhyay, R. Ali-Fehmi, T. J. Mangner, P. K. Chakraborty, S. Mittal, O. Muzik. *Nucl. Med. Biol.*, **39**, 926 (2012)
100. D. O. Kamson, S. Mittal, A. Buth, O. Muzik, W. J. Kupsky, N. L. Robinette, G. R. Barger, C. Juhász. *Mol. Imaging*, **12**, 327 (2013)
101. C. Juhász, S. Dwivedi, D. O. Kamson, S. K. Michelhaugh, S. Mittal. *Mol. Imaging*, **13**, 7290.2014.00015 (2014)

102. D.-Y. Hou, A. J. Muller, M. D. Sharma, J. DuHadaway, T. Banerjee, M. Johnson, A. L. Mellor, G. C. Prendergast, D. H. Munn. *Cancer Res.*, **67**, 792 (2007)
103. E. Fox, T. Oliver, M. Rowe, S. Thomas, Y. Zakharia, P. B. Gilman, A. J. Muller, G. C. Prendergast. *Front. Oncol.*, **8**, Article 370 (2018)
104. T. Komiya, C. H. Huang. *Front. Oncol.*, **8**, Article 423 (2018)
105. L. Xie, J. Maeda, K. Kumata, J. J. Yui, Y. D. Zhang, A. Hatori, N. Nengaki, H. Wakizaka, M. Fujinaga, T. Yamasaki, Y. Shimoda, M. Higuchi, T. Suhara, F. Wang, M. R. Zhang. *Sci. Rep.*, **5**, 16417 (2015)
106. F. Anquetil, G. Mondanelli, N. Gonzalez, T. Rodriguez Calvo, J. Zapardiel Gonzalo, L. Krogvold, K. Dahl-Jørgensen, B. Van den Eynde, C. Orabona, U. Grohmann, M. G. von Herrath. *Diabetes*, **67**, 1858 (2018)
107. H. H. Coenen, in *PET Chemistry: The Driving Force in Molecular Imaging. Ernst Schering Research Foundation Workshop 62*, ed. P. A. Schubiger, L. Lehmann,M. Friebe, Springer-Verlag, Berlin Heidelberg, 2007, pp. 15
108. P. W. Miller, N. J. Long, R. Vilar, A. D. Gee. *Ang. Chem. Int. Ed.*, **47**, 8998 (2008)
109. S. Preshlock, M. Tredwell, V. Gouverneur. *Chem. Rev.*, **116**, 719 (2016)
110. H. H. Coenen, J. Ermert. *Clin. Transl. Imaging*, **6**, 169 (2018)
111. W. W. Moses. *Nucl. Instrum. Methods Phys. Res., Sect. A*, **648, Supplement 1**, S236 (2011)
112. A. Sanchez-Crespo, P. Andreo, S. A. Larsson. *Eur. J. Nucl. Med. Mol. Imaging*, **31**, 44 (2004)
113. R. Chirakal, B. G. Sayer, G. Firnau, E. S. Garnett. *J. Labelled Compd. Radiopharm.*, **25**, 63 (1988)
114. R. Li, S.-C. Wu, S.-C. Wang, Z. Fu, Y. Dang, L. Huo. *Appl. Rad. Isot.*, **68**, 303 (2010)
115. A. Abbas, C. Beamish, R. McGirr, J. Demarco, N. Cockburn, D. Krokowski, T. Lee, M. Kovacs, M. Hatzoglou, S. Dhanvantari. *F1000Research*, **5**, (2016)
116. S. D. Krämer, L. Mu, A. Müller, C. Keller, O. F. Kuznetsova, C. Schweinsberg, D. Franck, C. Müller, T. L. Ross, R. Schibli, S. M. Ametamey. *J. Nucl. Med*, **53**, 434 (2012)
117. T. Sun, G. Tang, H. Tian, X. Wang, X. Chen, Z. Chen, S. Wang. *Appl. Rad. Isot.*, **70**, 676 (2012)
118. J. Henrottin, C. Lemaire, D. Egrise, A. Zervosen, B. Van den Eynde, A. Plenevaux, X. Franci, S. Goldman, A. Luxen. *Nucl. Med. Biol.*, **43**, 379 (2016)
119. T. K. Venkatachalam, D. H. R. Stimson, G. K. Pierens, R. Bhalla, D. C. Reutens. *Appl. Rad. Isot.*, **131**, 41 (2018)
120. I. H. Shih, X.-D. Duan, F.-L. Kong, M. D. Williams, K. Yang, Y.-H. Zhang, D. J. Yang. *BioMed Res. Int.*, **2014**, 492545 (2014)
121. A. Chiotellis, L. Mu, A. Müller, S. V. Selivanova, C. Keller, R. Schibli, S. D. Krämer, S. M. Ametamey. *Eur. J. Med. Chem.*, **70**, 768 (2013)
122. K.-J. Langen, N. Galldiks, E. Hattingen, N. J. Shah. *Nat. Rev. Neurol.*, **13**, 279 (2017)
123. A. Chiotellis, A. Müller Herde, S. L. Rössler, A. Brekalo, E. Gedeonova, L. Mu, C. Keller, R. Schibli, S. D. Krämer, S. M. Ametamey. *J. Med. Chem.*, **59**, 5324 (2016)
124. Y. Xin, H. Cai. *Mol. Imaging Biol.*, **19**, 589 (2016)
125. Y. Xin, X. Gao, L. Liu, W.-P. Ge, M. K. Jain, H. Cai. *Mol. Imaging Biol.*, **21**, 1138 (2019)
126. S. K. Michelhaugh, O. Muzik, A. R. Guastella, N. V. Klinger, L. A. Polin, H. C. Cai, Y. C. Xin, T. J. Mangner, S. H. Zhang, C. Juhasz, S. Mittal. *J. Nucl. Med*, **58**, 208 (2017)
127. Y. Xin, X. Yue, H. Li, Z. Li, H. Cai, A. K. Choudhary, S. Zhang, D. C. Chugani, S. A. Langhans. *Sci. Rep.*, **10**, 3800 (2020)

128. G. Balz, G. Schiemann. *Chem. Ber.*, **60**, 1186 (1927)
129. A. J. Palmer, J. C. Clark, R. W. Goulding. *Int. J. Appl. Radiat. Isot.*, **28**, 53 (1977)
130. H. L. Atkins, D. R. Christman, J. S. Fowler, W. Hauser, R. M. Hoyte, J. F. Klopper, S. S. Lin, A. P. Wolf. *J. Nucl. Med*, **13**, 713 (1972)
131. P. S. Weiss, J. Ermert, J. Castillo Meleán, D. Schäfer, H. H. Coenen. *Bioorg. Med. Chem.*, **23**, 5856 (2015)
132. R. Fitzi, D. Seebach. *Tetrahedron*, **44**, 5277 (1988)
133. E. Lee, A. S. Kamlet, D. C. Powers, C. N. Neumann, G. B. Boursalian, T. Furuya, D. C. Choi, J. M. Hooker, T. Ritter. *Science*, **334**, 639 (2011)
134. E. Lee, J. M. Hooker, T. Ritter. *J. Am. Chem. Soc.*, **134**, 17456 (2012)
135. H. Ren, H. Y. Wey, M. Strebl, R. Neelamegam, T. Ritter, J. M. Hooker. *ACS Chem. Neurosci.*, **5**, 611 (2014)
136. B. D. Zlatopolskiy, J. Zischler, E. A. Urusova, H. Endepols, E. Kordys, H. Frauendorf, F. M. Mottaghy, B. Neumaier. *ChemistryOpen*, **4**, 457 (2015)
137. N. Ichiishi, A. F. Brooks, J. J. Topczewski, M. E. Rodnick, M. S. Sanford, P. J. H. Scott. *Org. Lett.*, **16**, 3224 (2014)
138. M. Tredwell, S. M. Preshlock, N. J. Taylor, S. Gruber, M. Huiban, J. Passchier, J. Mercier, C. Génicot, V. Gouverneur. *Ang. Chem. Int. Ed.*, **53**, 7751 (2014)
139. A. V. Mossine, A. F. Brooks, K. J. Makaravage, J. M. Miller, N. Ichiishi, M. S. Sanford, P. J. H. Scott. *Org. Lett.*, **17**, 5780 (2015)
140. K. J. Makaravage, A. F. Brooks, A. V. Mossine, M. S. Sanford, P. J. H. Scott. *Org. Lett.*, **18**, 5440 (2016)
141. S. J. Lee, K. J. Makaravage, A. F. Brooks, P. J. H. Scott, M. S. Sanford. *Ang. Chem. Int. Ed.*, **58**, 3119 (2019)
142. B. D. Zlatopolskiy, J. Zischler, P. Krapf, F. Zarrad, E. A. Urusova, E. Kordys, H. Endepols, B. Neumaier. *Chem. - Eur. J.*, **21**, 5972 (2015)
143. R. Richarz, P. Krapf, F. Zarrad, E. A. Urusova, B. Neumaier, B. D. Zlatopolskiy. *Org. Biomol. Chem.*, **12**, 8094 (2014)
144. D. Schäfer, P. Weiß, J. Ermert, J. Castillo Meleán, F. Zarrad, B. Neumaier. *Eur. J. Org. Chem.*, **2016**, 4621 (2016)
145. J. Zischler, N. Kolks, D. Modemann, B. Neumaier, B. D. Zlatopolskiy. *Chem. - Eur. J.*, **23**, 3251 (2017)
146. B. D. Zlatopolskiy, J. Zischler, D. Schäfer, E. A. Urusova, M. Guliyev, O. Bannykh, H. Endepols, B. Neumaier. *J. Med. Chem.*, **61**, 189 (2018)
147. R. P. Loach, O. S. Fenton, K. Amaike, D. S. Siegel, E. Ozkal, M. Movassaghi. *J. Org. Chem.*, **79**, 11254 (2014)
148. T. Tang, H. S. Gill, A. Ogasawara, J. N. Tinianow, A. N. Vanderbilt, S.-P. Williams, G. Hatzivassiliou, S. White, W. Sandoval, K. DeMent, M. Wong, J. Marik. *Nucl. Med. Biol.*, **51**, 10 (2017)
149. B. C. Giglio, H. Fei, M. Wang, H. Wang, L. He, H. Feng, Z. Wu, H. Lu, Z. Li. *Theranostics*, **7**, 1524 (2017)
150. N. Galldiks, K. J. Langen. *Q. J. Nucl. Med. Mol. Imaging*, **59**, 70 (2015)
151. A. Habermeier, J. Graf, B. F. Sandhöfer, J.-P. Boissel, F. Roesch, E. I. Closs. *Amino Acids*, **47**, 335 (2015)
152. Y. D. Bhutia, E. Babu, V. Ganapathy. *Biochim. Biophys. Acta*, **1848**, 453 (2015)
153. M. T. Travers, I. F. Gow, M. C. Barber, J. Thomson, D. B. Shennan. *Biochim. Biophys. Acta*, **1661**, 106 (2004)
154. V. P. Pai, A. M. Marshall, L. L. Hernandez, A. R. Buckley, N. D. Horseman. *Breast Cancer Res*, **11**, R81 (2009)

155. J. M. Leeds, P. J. Brown, G. M. McGeehan, F. K. Brown, J. S. Wiseman. *J. Biol. Chem.*, **268**, 17781 (1993)
156. M. Sono, M. P. Roach, E. D. Coulter, J. H. Dawson. *Chem. Rev.*, **96**, 2841 (1996)
157. D. Ribatti. *Experimental Cell Research*, **328**, 314 (2014)
158. H. Y. Kim, J. Y. Lee, Y.-S. Lee, J. M. Jeong. *J. Labelled Compd. Radiopharm.*, **62**, 566 (2019)
159. D.-B. Su, J.-X. Duan, Q.-Y. Chen. *Tetrahedron Lett.*, **32**, 7689 (1991)

8. List of Abbreviations

1-FETrp	1-(2-Fluoroethyl)tryptophan
1MTrp	N_{in}-Methyltryptophan
2-CF_3-Trp	2-Trifluoromethyltryptophan
3-HANA	3-Hydroxyanthranillic acid
3-HAO	3-Hydroxyanthranilate oxidase
3-HK	3-Hydroxykynurenine
5-OH-4-FTrp	5-Hydroxy-4-fluorotryptophan
5-OH-6-FTrp	5-Hydroxy-6-fluorotryptophan
5-HIAA	5-Hydroxy-3-indolacetic acid
5-HIAL	5-Hydroxy-3-indolacetaldehyde
5-HT	Serotonin
5-HTOL	5-hydroxytryptophol
5-OH-Trp	5-Hydroxytryptophan
α7nACh Receptor	α7 Nicotinic acetylcholine receptor
γITF	Interferon-γ
AADC	Aromatic amino acid decarboxylase
ADH	Alcohol dehydrogenase
Ala	Alanine
ALDH2	Aldehyde dehydrogenase type 2
ALDR	Aldehyde reductase
AMT	α-Methyltryptophan
ArBPin	Aryl pinacol boronate
ASC	Alanine-, serine-, and cysteine-preferring transporter system
BH_4	Tetrahydrobiopterin

Boc	*tert*-Butyloxycarbonyl
c.a.	Carrier added
CAM model	Chicken chorioallantoic membrane model
CAT	Catalase
*c*GMP	GMP (good manufacturing practice) conform
CT	Computed tomography
DAO	D-Amino acid oxidase
DMA	*N*,*N*-Dimethylacetamide
DMF	*N*,*N*-Dimethylformamide
ee	Enantiomeric excess
Et	Ethyl
FET	*O*-(2-Fluoroethyl)tyrosine
FTrp	Fluorotryptophan
FETrp	1-(2-Fluoroethyl)tryptophan
GBq	Gigabecquerel
GCH1	GTP-cyclohydroxylase-1
GE	General Electrics
GPT	Glutamic pyruvic transaminase
HIOMT	Hydroxyindole *O*-methyltransferase
HPLC	High-performance liquid chromatography
IDO	Indoleamine 2,3-dioxygenase
Indoximod	D-1MTrp; D-N_{in}-Methyltryptophan
ITrp	Iodotryptophan
K2.2.2	4,7,13,16,21,24-Hexaoxa-1,10-diazabicyclo[8.8.8]hexacosane
KAT	Kynurenine aminotransferases
keV	Kiloelectron-volt
K_m	Michaelis-Menten constant
KMO	Kynurenine 3-monooxygenase
KYN	Kynurenine
KYNA	Kynurenic acid
KYNU	Kynureninase

LAT	L-Amino acid transporter
LC/MS	Liquid chromatography–mass spectrometry
LDA	Lithium diisopropylamide
MAO	Monoamine oxidase
MBq	Megabecquerel
MeCN	Acetonitrile
Me	Methyl
MeOH	Methanol
µPET	microPET
MRI	Magnetic resonance imaging
N_{in}	Nitrogen of the indole ring
NAD^+	Nicotinamide adenine dinucleotide, oxidized form
NAS	*N*-Acetylserotonin
NAT	Serotonin *N*-acetyltransferase
*n*BuOH	Butanol-1
n.c.a	No carrier added
n.d.c.	Non-decay corrected
NLG919	α-Cyclohexyl-5*H*-imidazo[5,1-a]isoindole-5-ethanol
NMDA	*N*-Methyl-D-aspartate
PET	Positron emission tomography
PiB	Pittsburgh Compound B; 2-(4'-methylaminophenyl)-6-hydroxybenzothiazole
Quin	Quinolinic acid
RCC	Radiochemical conversion; RCC refers to the amount of radiofluoride which is transformed to the desired 18F-labeled compound. It is determined by radio-HPLC or radio-TLC
RCY	Radiochemical yield; RCY refers to the isolated yield of the radiochemically and chemically pure radiolabeled compound
S_N2	Bimolecular aliphatic nucleophilic substitution
S_NAr	Aromatic nucleophilic substitution
SPE	Solid phase extraction

*t*Bu	*tert*-Butyl
TBAF	Tetrabutylammonium fluoride
TDO	Tryptophan-2,3-dioxygenase
TEAF	Tetraethylammonium fluoride
TFA	Trifluoroacetic acid
TMEDA	*N*,*N*,*N*',*N*'-Tetramethylethylendiamine
TPH	Tryptophan hydroxylase
Trp	Tryptophan
TSPO	Translocator protein 18 kDa
V_{max}	Maximal velocity of the reaction
Z-(*R*)-BMI	(*R*)-(+)-1-(Benzyloxycarbonyl)-2-*tert*-butyl-3-methyl-4-imidazolidinone